Synthesis and Characterization of Tris(bipyridyl)ruthenium(II)-Modified Mono-, Di-, and Trinuclear Manganese Complexes as Electron-Transfer Models for Photosystem II

Dirk Burdinski, Eberhard Bothe, and Karl Wieghardt*

Max-Planck Institut für Strahlenchemie, Stiftstrasse 34-36, D-45470 Mülheim, Germany

Received June 29, 1999

With the aim of modeling the arrangement of redox-active and photoactive components along the electron-transfer pathway of photosystem II, tetra- to nonanuclear transition metal complexes have been synthesized, comprising one, two, or three manganese ions, oxidizable phenolates, and tris(2,2′-bipyridyl)ruthenium(II)-type units as photosensitizers. These model complexes are considered to be mononuclear ($[L^nMn](PF_6)_m$), dinuclear ($[L^{1a}Mn^{IV}{}_2(\mu\text{-}O)_2](PF_6)_6$), or trinuclear ($[L^nMn^{II}Mn^{II}Mn^{II}L^n](PF_6)_{12}$) with respect to the number of manganese centers present. Electronic coupling between the manganese ions is strongly antiferromagnetic in the case of the di(μ-oxo)-dimanganese compound $[L^{1a}Mn^{IV}{}_2(\mu\text{-}O)_2](PF_6)_6$, where the "ligand" $[H_2L^{1a}]^{4+}$ consists of two tris(bipyridyl)-ruthenium(II)-type units covalentely bound to a bismacrocyclic Me_2dtne backbone to which the manganese ions are coordinated via an additional phenolate oxygen (Me_2dtne = 1,2-bis(4-methyl-1,4,7-triazacyclononyl)ethane). Weak antiferromagnetic coupling is observed in compounds $[L^nMn^{II}Mn^{II}Mn^{II}L^n](PF_6)_{12}$, where the three metals are in a linear arrangement (face-sharing octahedral). They are bridged by three phenolate oxygens of each of the deprotonated "ligands" $[H_3L^n]^{6+}$, respectively. Each ligand $[H_3L^n]^{6+}$ (n = 1, 2) consists of a tacn ring with three pendent arm phenols which are each bound to a tris(bipyridyl)ruthenium(II)-type unit (tacn = 1,4,7-triazacyclononane). In these compounds several electron-transfer steps were detected by electrochemical methods which are assigned to different redox processes located at individual electrochemically active components (Mn, Ru, bipyridyl, phenolate). For example, in the "mononuclear" compounds $[L^nMn](PF_6)_m$ (n = 1 or 2) Mn(II), Mn(III), and Mn(IV) are accessible and three Ru(II) centers are reversibly oxidized to Ru(III), and in addition, the coordinated phenolate can be oxidized to a highly reactive, coordinated phenoxyl radical. In several cases very slow heterogeneous electron-transfer rates were observed for redox processes involving the manganese centers.

Introduction

Photosynthesis is one of the basic processes in nature. A detailed knowledge of the underlying mechanism on a molecular level is important for a deeper understanding of the biochemical principles, which allows one to develop artificial systems. Conversion of the energy of light as a cheap energy source to chemical energy is the goal. Interest in the design of artificial systems using solar energy has arisen within the past few years.[1−3] The detailed molecular structure and the mechanism of action of the biological photosynthetic machine still remains largely to be determined. The design of a suitable artificial system is the major aim of the project described in this paper.

In the biological photosynthetic system, the energy of light is used to transfer electrons from water to carbon dioxide, which is reduced to energy-rich organic compounds ("biomass"). Water oxidation as the source of these electrons and protons is performed in photosystem II (PS II).[4−7] This large membrane-bound protein complex consists of an extended light-absorbing antenna system including the reaction center P680, which consists of a special arrangement of two chlorophylls as the location of the initial light-driven charge separation. Energy-rich electrons generated by the absorption of a quantum of light by the reaction center are transferred by several quinones to the acceptor site of PS II and further on to PS I. In this process an electron hole is generated at the primary donor P680, which is now a strong oxidant and oxidizes a nearby tyrosine (Y_Z) residue to a neutral, deprotonated phenoxyl radical ($Y_Z^{\bullet}$); effective deprotonation of this phenol/phenoxyl species is supported by hydrogen bonding to a nearby histidine residue.[8,9] The phenoxyl radical acts as an one-electron oxidant of a tetranuclear manganese cluster. In a stepwise fashion, four oxidation equivalents are accumulated as the process is repeated. The fourth oxidation step initiates the evolution of a dioxygen molecule resulting from the oxidation of two water molecules, which have probably been coordinatively bound to the manganese cluster. These water molecules are the ultimate electron source of the overall process.

The manganese cluster is believed to consist of a dimer of di(μ-oxo)dimanganese dimers, in which the manganese ions reversibly cycle between the oxidation states +II, +III, and +IV.[10−12] The nature of the interaction of the manganese cluster

(1) Rüttinger, W.; Dismukes, G. C. *Chem. Rev.* **1997**, *97*, 1−24.
(2) Balzani, V.; Campagna, S.; Denti, G.; Juris, A.; Serroni, S.; Venturi, M. *Solar Energy Mater. Solar Cells* **1995**, *38*, 159−173.
(3) Amouyal, E. *Solar Energy Mater. Solar Cells* **1995**, *38*, 249−276.
(4) Diner, B. A.; Babcock, G. T. In Diner, B. A., Babcock, G. T., Eds.; Kluwer: Dordrecht, The Netherlands, 1996; p 213.
(5) Svensson, B.; Etchebest, C.; Tuffery, P.; Kan, P. v.; Smith, J.; Styring, S. *Biochemistry* **1996**, *35*, 14486−14502.
(6) Vermaas, W. F. J.; Styring, S.; Schröder, W. P.; Andersson, B. *Photosynth. Res.* **1993**, *38*, 249−263.
(7) Debus, R. J. *Biochim. Biophys. Acta* **1992**, *1102*, 269−352.
(8) Hays, A.-M. A.; Vassiliev, I. R.; Goldbeck, J. H.; Debus, R. J. *Biochemistry* **1998**, *37*, 11352−11365.
(9) Mamedov, F.; Sayre, R. T.; Styring, S. *Biochemistry* **1998**, *37*, 14245−14256.
(10) Iuzzolino, L.; Dittmer, J.; Dörner, W.; Meyer-Klaucke, W.; Dau, H. *Biochemistry* **1998**, *37*, 17112−17119.
(11) Penner-Hahn, J. E. *Struct. Bonding* **1998**, *90*, 1−36.

10.1021/ic990755a CCC: $19.00
Published on Web 12/18/1999

with the intermediate phenoxyl radical $Y_Z^{\bullet}$ during the electron-transfer and water oxidation reactions is not yet fully understood. However, recent results indicate a concerted proton−electron-transfer (H-atom abstraction) mechanism of the manganese-bound water molecules by the tyrosine radical.[13−20]

Our earlier studies on *structural models* of PS II and *structural and functional* models of other metallo enzymes with phenoxyl type radicals in the active site led us to investigate strategies for the development of *functional models* of PS II.[21−23] We concentrate on the design of an artificial system modeling the initial charge separation and the electron-transfer chain from the manganese cluster to the reaction center P680. To mimic the photoactive reaction center, complexes of the tris(bipyridyl)-ruthenium(II) type were chosen, because of their well-understood photophysical properties.[24] A similar strategy has recently been employed by others, proving this complex to be a good model for the initial, light-driven charge separation process. Light-induced *intra*molecular electron transfer has been observed from a covalently bound phenol and in another model complex from a manganese(II) ion to the photogenerated ruthenium(III) center.[25,26] Also, an *inter*molecular electron transfer involving a dinuclear manganese complex has recently been described.[27]

Here we present synthetic strategies for the *covalent linkage* of the $Ru(bpy)_3$-type unit to the *multinuclear manganese cluster* as an integral part of supramolecular model compounds both with and without a phenolate moiety as part of the bridging unit. In the latter case the principal arrangement of the redox-active components mimics that of PS II. This compound represents the first example of a model compound consisting of an artificial reaction center covalently bound to a multinuclear manganese cluster bridged by a redox-active phenolate. After submission of this paper a report describing a similar system appeared in the literature.[25b]

Results and Discussion

Synthesis. To synthetically build an assembly consisting of a dinuclear di(μ-oxo)dimanganese complex and photoactive units of the $Ru(bpy)_3$ type, a ligand system based on the bismacrocycle dtne (dtne = 1,2-bis(1,4,7-triazacyclononyl)-ethane) was developed, because this ligand is known to stabilize the desired $Mn_2(\mu\text{-}O)_2$ unit.[28,29] Preliminary experiments showed that dicationic $Ru(bpy)_3$ units linked via $(CH_2)_n$ groups to the bismacrocycle decrease the affinity of the dtne part toward manganese ions to the extent that formation of the desired manganese complexes does not occur.[30] To decrease the overall charge of the $Ru(bpy)_3$-containing pendent arm and to increase the affinity of the ligand system toward manganese ions, a phenolato-type oxygen donor was added to the $Ru(bpy)_3$-type unit. With the octahedral manganese ions being coordinated by three dtne nitrogens and the two expected oxo bridges, only one binding site for the coordination of one pendent arm would thus be available at each manganese center.

To achieve the introduction of only two additional functionalities to the dtne ligand, the dimethylated derivative Me_2dtne (**3**) was prepared by sodium borohydride reduction of the amidinium salt **2** (Scheme 1).[31] The phenOH pendent arm was introduced in a Mannich-type reaction by isolating the di(methoxymethyl) adduct formed in the reaction of Me_2dtne with paraformaldehyde in methanol and treating this with phenOH in refluxing toluene.[32−34] The two $Ru(bpy)_3$-type units were completed by reacting compound **5** with 3 equiv of *cis*-$[(bpy)_2RuCl_2]$, yielding the PF_6 salt of the ligand $[H_2L^{1a}]^{4+}$ after precipitation from the pure chromatographic fractions containing the respective chloride salt using NH_4PF_6. Although no high-resolution ^1H NMR spectra could be obtained of this compound (possibly due to strong intramolecular hydrogen bonding), the ratio of aromatic to aliphatic protons corresponds to the expected value (22:19). The observed electrospray ionization mass spectrometry (ESI-MS) signal at $m/z = 311$ results from thermal dehydroamination reaction of the pendent arm groups *during the measurement*. This has been shown to be true by performing the decomposition in refluxing aqueous ethanol and identifying the dehydroamination product by thin-layer chromatography (TLC) and ESI-MS independently. The decomposition products had not been present in the material used for the above ESI-MS measurement.

The PF_6 salt of the $[H_2L^{1a}]^{4+}$ ligand is soluble in acetonitrile and acetone and almost insoluble in ethanol, but it can be solubilized in the latter solvent by addition of a small amount of acetone to give a clear red solution. Addition of manganese(III) acetate induced a color change to deep brown, and after precipitation with NH_4PF_6 a brown powder was obtained. The brown solution of this powder in an acidic (HPF_6) ethanol/

(12) Yachandra, V. K.; Sauer, K.; Klein, M. P. *Chem. Rev.* **1996**, *96*, 2927−2950.
(13) Limburg, J.; Szalai, V. A.; Brudvig, G. W. *J. Chem. Soc., Dalton Trans.* **1999**, 1353−1361.
(14) Diner, B. A.; Force, D. A.; Randall, D. W.; Britt, R. D. *Biochemistry* **1998**, *37*, 17931−17943.
(15) Szalai, V. A.; Kühne, H.; Lakshmi, K. V.; Brudvig, G. W. *Biochemistry* **1998**, *37*, 13594−13603.
(16) Tommos, C.; Babcock, G. T. *Acc. Chem. Res.* **1998**, *31*, 18−25.
(17) Hoganson, C. W.; Babcock, G. T. *Science* **1997**, *277*, 1953−1956.
(18) Tommos, C.; Tang, X.-S.; Warncke, K.; Hoganson, C. W.; Styring, S.; McCracken, J.; Diner, B. A.; Babcock, G. T. *J. Am. Chem. Soc.* **1995**, *117*, 10325−10335.
(19) Hoganson, C. W.; Lydakis-Simantiris, N.; Tang, X.-S.; Tommos, C.; Warnke, K.; Babcock, G. T.; Diner, B. A.; McCracken, J.; Styring, S. *Photosynth. Res.* **1995**, *46*, 177−184.
(20) Gilchrist, M. L.; Ball, J. A.; Randall, D. W.; Britt, R. D. *Proc. Natl. Acad. Sci. U.S.A.* **1995**, *92*, 9545−9549.
(21) Chaudhuri, P.; Hess, M.; Flörke, U.; Wieghardt, K. *Angew. Chem.* **1998**, *110*, 2340−2343.
(22) Sokolowski, A.; Leutbecher, H.; Weyhermüller, T.; Schnepf, R.; Bothe, E.; Bill, E.; Hildebrandt, P.; Wieghardt, K. *J. Biol. Inorg. Chem.* **1997**, *2*, 444−453.
(23) Adam, B.; Bill, E.; Bothe, E.; Goerdt, B.; Haselhorst, G.; Hildenbrand, K.; Sokolowski, A.; Steenken, S.; Weyhermüller, T.; Wieghardt, K. *Chem. Eur. J.* **1997**, *3*, 308−319.
(24) Balzani, V.; Scandola, F. *Supramolecular Photochemistry*; Ellis Horwood: New York, 1991.
(25) (a) Magnuson, A.; Berglund, H.; Koral, P.; Hammarström, L.; Åkermark, B.; Styring, S.; Sun, L. *J. Am. Chem. Soc.* **1997**, *119*, 10720−10725. (b) Sun, L.; Burkitt, M.; Tamm, M.; Raymond, M. K.; Abrahamsson, M.; LeGourrierec, D.; Frapart, Y.; Magnuson, A.; Kenez, P. H.; Brandt, P.; Tran, A.; Hammarström, L.; Styring, S.; Akermark, B. *J. Am. Chem. Soc.* **1999**, *121*, 6834.
(26) Sun, L.; Berglund, H.; Davydov, R.; Norrby, T.; Hammarström, L.; Korall, P.; Börje, A.; Philouze, C.; Berg, K.; Tran, A.; Anderson, M.; Stenhagen, G.; Mårtensson, J.; Almgren, M.; Styring, S.; Åkermark, B. *J. Am. Chem. Soc.* **1997**, *119*, 6996−7004.
(27) Magnuson, A.; Frapart, Y.; Abrahamsson, M.; Horner, O.; Åkermark, B.; Sun, L.; Girerd, J.-J.; Hammarström, L.; Styring, S. *J. Am. Chem. Soc.* **1999**, *121*, 89−96.
(28) Schäfer, K.-O.; Bittl, R.; Zweigert, W.; Lendzian, F.; Haselhorst, G.; Weyhermüller, T.; Wieghardt, K.; Lubitz, W. *J. Am. Chem. Soc.* **1998**, *120*, 13104−13120.
(29) Weyhermüller, T. Dissertation, Ruhr-Universität Bochum, 1994.
(30) Burdinski, D. Dissertation, Ruhr-Universität Bochum, 1998.
(31) Alder, R. W.; Mowlam, R. W.; Vachon, D. J.; Weisman, G. R. *J. Chem. Soc., Chem. Commun.* **1992**, 507−508.
(32) Lukyanenko, N. G.; Pastushok, V. N.; Bordunov, A. V. *Synthesis* **1991**, 241−242.
(33) Lukyanenko, N. G.; Pastushok, V. N.; Bordunov, A. V.; Vetrogon, V. I.; Vetrogon, N. I.; Bradshaw, J. S. *J. Chem. Soc., Perkin Trans. 1* **1994**, 1489−1493.
(34) Bordunov, A. V.; Bradshaw, J. S.; Zhang, X. X.; Dalley, N. K.; Kou, X.; Izatt, R. M. *Inorg. Chem.* **1996**, *35*, 7229−7240.

Scheme 1[a]

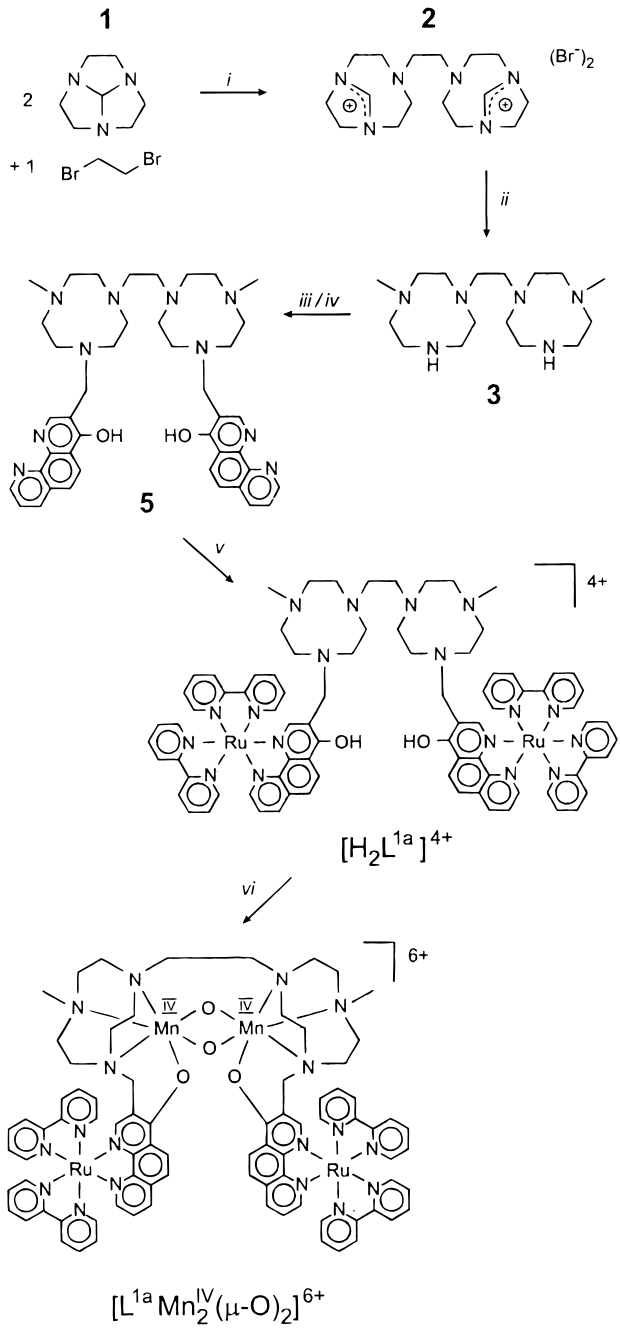

[a] Experimental conditions: (i) CH_3CN, room temperature (rt), 1 week; (ii) $NaBH_4$, MeOH, reflux; (iii) $(CH_2O)_x$, MeOH, rt, overnight; (iv) phenOH, toluene, reflux, 48 h; (v) *cis*-$[(bpy)_2RuCl_2]\cdot 2H_2O$, MeOH, reflux, 48 h; (vi) "$Mn(ac)_3$", H_2O_2, HPF_6, ethanol/acetone, rt.

Scheme 2[a]

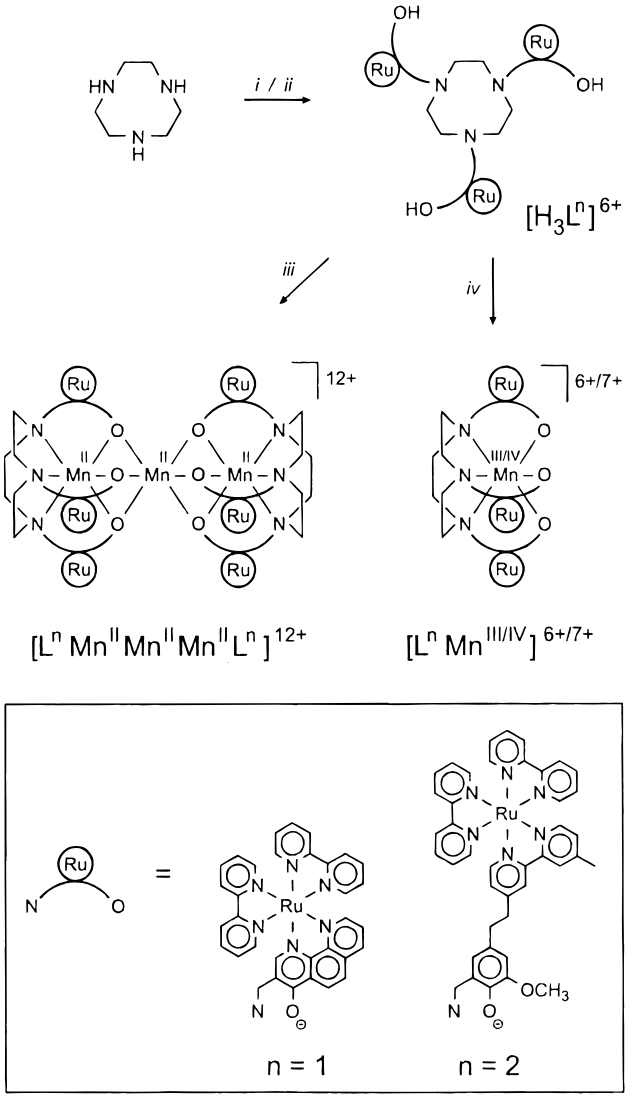

[a] Experimental conditions: (i) $n = 1$, $(CH_2O)_x$, MeOH, rt, overnight, then phenOH, toluene, reflux, 48 h; $n = 2$, $(CH_2O)_x$, MeOH, reflux, 72 h; (ii) *cis*-$[(bpy)_2RuCl_2]\cdot 2H_2O$, MeOH, reflux; (iii) manganese(III) acetate, ethanol/acetone, ascorbic acid, NaOMe, rt; (iv) "$Mn(ac)_3$", ethanol/acetone, H_2O_2, HPF_6.

acetone mixture reacted with hydrogen peroxide, yielding a deep green solution from which almost black microcrystals of $[L^{1a}Mn^{IV}{}_2(\mu\text{-}O)_2](PF_6)_6$ were obtained. The coordination of the ligand to the Mn_2O_2 core increases the thermal stability of the molecule to such an extent that the intact molecule could be readily detected by ESI-MS. It is noted that the observed peaks belong to the one-electron-reduced pentacationic form of the molecule.

$[H_3L^1]^{6+}$ is the tacn derivative (tacn = 1,4,7-triazacyclononane) bearing three pendent arms of the $Ru(bpy)_3$ type based on a CH_2-linked phenOH group (Scheme 2). This ligand was prepared as its PF_6 salt in a reaction series analogous to that described for the $[H_2L^{1a}]^{4+}$ ligand from the starting materials 1,4,7-triazacyclononane, paraformaldehyde, and phenOH and then *cis*-$[(bpy)_2RuCl_2]$. The only observed ESI-MS signal at $m/z = 311$ for this ligand corresponds to the mononuclear fragment already described for $[H_2L^{1a}](PF_6)_4$, which again has been shown not to be present in the starting material. The ^1H NMR spectrum shows the expected ratio of broad aromatic to aliphatic proton signals (22:6). $[H_3L^1](PF_6)_6$ has analogous solubility properties as the Me_2dtne derivative. The red color of the solution of the ligand in ethanol/acetone changed to brown upon addition of manganese(III) acetate. TLC studies indicated the formation of two new compounds in solution. By using oxidative reaction conditions (HPF_6/H_2O_2), the equilibrium between the two shifted to only one product (to the one displaying lower TLC mobility). This complex was isolated by addition of NH_4PF_6 to the reaction mixture as brown microcrystalline $[L^1Mn^{III}](PF_6)_6$.

Isolation of the other product was achieved by using reductive conditions. In an argon blanketing atmosphere, the reaction

Chart 1

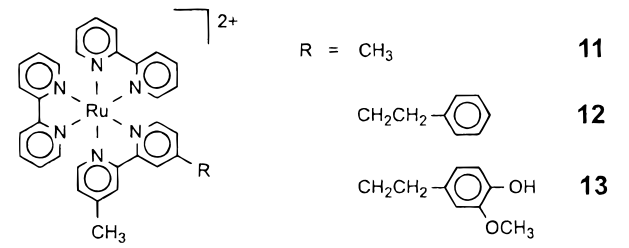

Scheme 3

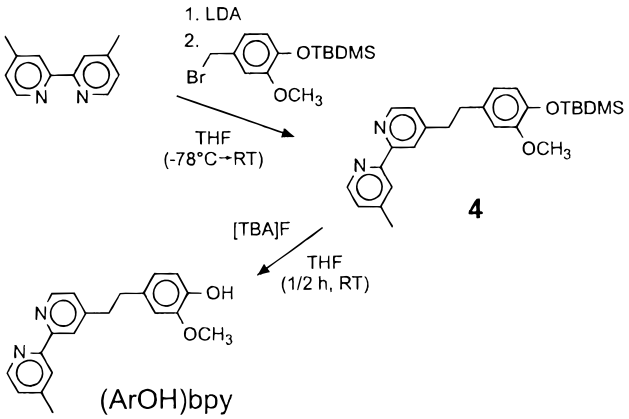

solution was treated with sodium methoxide and ascorbic acid, which induced a color change to bright red and allowed the isolation of red microcrystals of the trinuclear manganese complex $[L^1Mn^{II}Mn^{II}Mn^{II}L^1](PF_6)_{12}$. This species is the product with the higher TLC mobility which was originally observed in the reaction mixture. The formulation as a trinuclear complex is consistent with all physical properties of the compound (see below). The bridging of two mononuclear tris(phenolate)tacn metal complexes by a third metal ion as shown in Scheme 2 is well-known.[35,36] Heterotrinuclear complexes of this type such as a $Co^{III}Mn^{II}Co^{III}$ compound have also been previously isolated.[37]

Since electron transfer from the manganese cluster to the photoactive reaction center in PS II is mediated by a tyrosine residue, it appeared to be worthwhile to synthesize a molecule consisting of a photoactive unit, a manganese cluster, and a bridging phenol group to model the electron-transfer pathway in PS II. In other words, it was necessary to separate the phenol group from the $Ru(bpy)_3$-type unit, which are both combined within one ring system in the phenOH group of the $[H_3L^1]^{6+}$ ligand. Thus, we have synthesized compound **13** (Chart 1) bearing a phenol group covalentely linked to a $Ru(bpy)_3$-type unit via the reaction of *cis*-$[(bpy)_2RuCl_2]$ with the (ArOH)bpy ligand, which was obtained from 4,4′-dimethyl-2,2′-bipyridyl as shown in Scheme 3.

In a reaction series analogous to the synthesis of the $[H_3L^1]^{6+}$ ligand, the Mannich reaction was used to attach three (ArOH)-bpy units to a tacn ring via a methylene group.[23,38−40] The following treatment with 4 equiv of *cis*-$[(bpy)_2RuCl_2]$ yielded after chromatographic purification the desired $[H_3L^2]^{6+}$ ligand as its chloride salt. Upon addition of NH_4PF_6 to an aqueous solution of this compound, the respective PF_6 salt was obtained in good yield (Scheme 2).

The reaction of this ligand with manganese(III) acetate in ethanol/acetone induced in the presence of air a slow color change from red to deep green. From this solution the product $[L^2Mn^{IV}](PF_6)_7$ precipitated as the deep green PF_6 salt. In comparison with the complex $[L^1Mn^{III}](PF_6)_6$ containing an air-stable manganese(III) center, manganese(IV) is more strongly stabilized in the L^2 complex due to the increased σ-donor capability of the phenolic oxygen in the latter ligand system. By using reductive conditions (sodium methoxide, ascorbic acid, argon atmosphere), the trinuclear manganese complex $[L^2Mn^{II}$-$Mn^{II}Mn^{II}L^2](PF_6)_{12}$ with physical properties similar to those of the former L^1 complex was obtained as red microcrystals. As in the L^1 ligand system TLC allows one to readily distinguish between the mono- and trinuclear manganese complexes. In both cases the trinuclear (with respect to the number of Mn ions) complexes with a twice as large positive charge and more than twice the molecular mass show a remarkably higher TLC mobility than the corresponding mononuclear species.

Ruthenium complexes **11** and **12** (Chart 1) have been prepared as reference compounds for photophysical measurements by the reaction of *cis*-$[(bpy)_2RuCl_2]$ with the ligands Me_2-bpy and (Ph)bpy, respectively. The latter was obtained by the reaction of monolithiated Me_2bpy with benzyl chloride and subsequent purification by liquid column and preparative gas chromatography.

Electronic Structure. Variable-temperature magnetic susceptibilities of the complexes were measured in the range 2−290 K by using a SQUID magnetometer and an applied external field of 1.0 T. The experimental data, χ_{exp}, were corrected for underlying diamagnetism, χ_D, and temperature-independent paramagnetism, χ_{TIP}. χ_D was calculated by use of Pascal's tabulated constants, and χ_{TIP} is a fit parameter in the subsequent simulation and fitting processes, for which values of 800×10^{-6} $cm^3 \cdot mol^{-1}$ for the mononuclear, 900×10^{-6} $cm^3 \cdot mol^{-1}$ for the dinuclear, and 1800×10^{-6} $cm^3 \cdot mol^{-1}$ for the trinuclear manganese complexes were obtained. The effective magnetic moments, μ_{eff}, of the manganese complexes as a function of the temperature are shown in Figure 1; the parameters are listed in Table 1.

The effective magnetic moment of the dinuclear manganese complex $[L^{1a}Mn_2(\mu\text{-}O)_2](PF_6)_6$ decreases from 2.77 μ_B at 290 K to 0.56 μ_B at 2 K, indicating a strong antiferromagnetic coupling between the two manganese(IV) ions, yielding an $S_t = 0$ ground state. The coupling constant $J = -130$ cm^{-1} ($H = -2J\, S_1 \cdot S_2$, $S_1 = 3/2$, $S_2 = 3/2$) is typical for di(μ-oxo)-bridged dimanganese(IV) complexes.[28,41−43] As expected, the compound is EPR-silent.

The mononuclear complex $[L^1Mn](PF_6)_6$ possesses a weakly temperature-dependent magnetic moment of 5.23 μ_B at 290 K and 4.87 μ_B at 10 K characteristic of a mononuclear manganese-(III) species ($S = 2$). The sharp drop in the effective magnetic moment below 10 K was simulated by introducing a small zero-field splitting of $|D| = 3.5$ cm^{-1}. Despite this significant zero-field splitting, it has been possible to obtain an EPR signal in frozen acetonitrile/toluene solution at 10 K with g values of 8

(35) Auerbach, U.; Eckert, U.; Wieghardt, K.; Nuber, B.; Weiss, J. *Inorg. Chem.* **1990**, *29*, 938−944.
(36) Beissel, T.; Birkelbach, F.; Bill, E.; Glaser, T.; Kesting, F.; Krebs, C.; Weyhermüller, T.; Wieghardt, K.; Butzlaff, C.; Trautwein, A. X. *J. Am. Chem. Soc.* **1996**, *118*, 12376−12390.
(37) Auerbach, U.; Stockheim, C.; Weyhermüller, T.; Wieghardt, K.; Nuber, B. *Angew. Chem.* **1993**, *105*, 735−737.
(38) Moore, D. A.; Fanwick, P. E.; Welch, M. J. *Inorg. Chem.* **1989**, *28*, 1504−1506.
(39) Tramontini, M.; Angiolini, L. *Tetrahedron* **1990**, *46*, 1791−1837.
(40) Tramontini, M. *Synthesis* **1973**, 703.
(41) Manchanda, R.; Brudvig, G. M.; Crabtree, R. H. *Coord. Chem. Rev.* **1995**, *144*, 1−38.
(42) Thorp, H. H.; Brudvig, G. W. *New J. Chem.* **1991**, *15*, 479−490.
(43) Wieghardt, K. *Angew. Chem.* **1989**, *101*, 1179−1198.

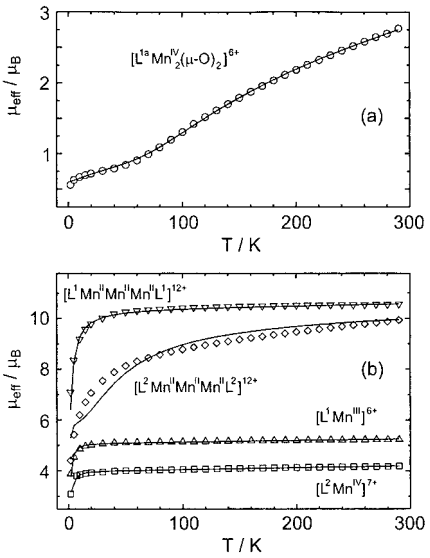

Figure 1. Temperature dependence of the magnetic moment of complexes $[L^{1a}Mn^{IV}{}_2(\mu\text{-}O)_2](PF_6)_6$ (a), $[L^1Mn^{III}](PF_6)_6$, $[L^2Mn^{IV}](PF_6)_7$, $[L^1Mn^{II}Mn^{II}Mn^{II}L^1](PF_6)_{12}$, and $[L^2Mn^{II}Mn^{II}Mn^{II}L^2](PF_6)_{12}$ (b).

Table 1. Magnetochemical Data of Complexes

complex	μ_{eff} (290 K)/μ_B	g	J [a]/cm^{-1}	D/cm^{-1}	S_t[b]
$[L^{1a}Mn^{IV}{}_2(\mu\text{-}O)_2]^{6+}$ [c]	2.77	2.0	−130		0
$[L^1Mn^{III}]^{6+}$	5.23	2.0		3.5	2
$[L^2Mn^{IV}]^{7+}$	4.19	2.0		5.1	3/2
$[L^1Mn^{II}Mn^{II}Mn^{II}L^1]^{12+}$	10.55	2.0	−0.2		5/2
$[L^2Mn^{II}Mn^{II}Mn^{II}L^2]^{12+}$	9.93	2.0	−2.5		5/2

[a] J represents the coupling constants between adjacent metal ions; in trinuclear complexes the coupling between the terminal metal ions is assumed to be zero (see the text). [b] Spin ground state. [c] In the fitting procedure a paramagnetic impurity (1%) with the assumed spin state $S = 5/2$ was considered.

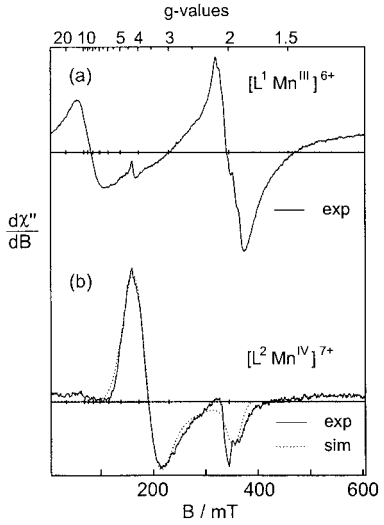

Figure 2. X-Band EPR spectra of complexes $[L^1Mn^{III}]^{6+}$ (a) and $[L^2Mn^{IV}]^{7+}$ (b) at 10 K in an acetonitrile/toluene (1:1 (v/v)) mixture (conditions: $\nu = 9.64$ GHz, microwave power 99 μW, modulation amplitude 12.8 G). Simulation with effective g values (b).

and 2, which are consistent with an integer spin system of $S = 2$ (Figure 2 a). The mononuclear complex $[L^2Mn](PF_6)_7$ is also EPR-active (Figure 2b); it displays a spectrum which was successfully simulated with effective g values of $g_\perp^{eff} = 3.95$ and $g_\parallel^{eff} = 1.95$ indicative of the $S = 3/2$ system of a manganese(IV) complex. This is confirmed by the only weakly temperature-dependent effective moment of the solid sample

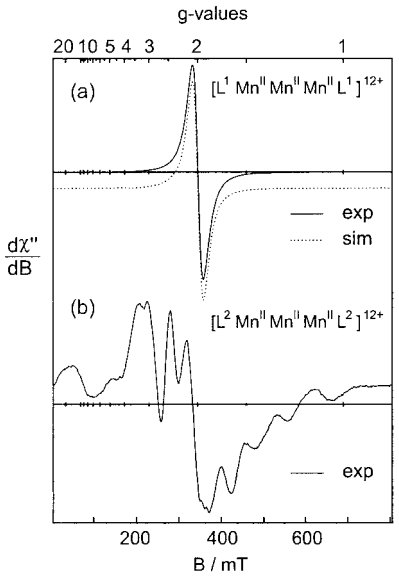

Figure 3. X-band EPR spectra of complexes $[L^1Mn^{II}Mn^{II}Mn^{II}L^1]^{12+}$ (a) and $[L^2Mn^{II}Mn^{II}Mn^{II}L^2]^{12+}$ (b) at 10 K in an acetonitrile/toluene (1:1 (v/v)) mixture (conditions: $\nu = 9.64$ GHz, microwave power 25 μW (a) and 99 μW (b), modulation amplitude 12.8 G). Simulation with a Lorentz function and $g = 1.99$ (a).

of 4.19 μ_B at 290 K, which slowly decreases to 3.85 μ_B at 10 K and then drops to 3.09 μ_B at 2 K. This behavior can again be simulated by introducing a significant zero-field splitting of $|D| = 5.1$ cm^{-1}.

Both trinuclear manganese complexes are weakly antiferromagnetically coupled. The observed μ_{eff} value at room temperature of 10.55 μ_B in the L^1 complex and of 9.93 μ_B in the L^2 complex is close to the calculated spin-only value of 10.25 μ_B for a system of three uncoupled manganese(II) ions. With decreasing temperature both decrease slowly to 7.09 and 4.41 μ_B at 2 K, respectively. This behavior is characteristic of a weak antiferromagnetic coupling between the central manganese and the two equivalent terminal manganese ions with coupling constants of −0.2 cm^{-1} ($[L^1Mn^{II}Mn^{II}Mn^{II}L^1](PF_6)_{12}$) and −2.5 cm^{-1} ($[L^2Mn^{II}Mn^{II}Mn^{II}L^2](PF_6)_{12}$). The coupling between the terminal manganese ions is assumed to be negligible and was therefore set to zero. No zero-field splitting was considered in the fitting procedure. This behavior is consistent with the observed EPR spectra (Figure 3), which show resonances around $g = 2$ for both complexes, indicating a very small zero-field splitting ($D \ll h\nu = 0.3$ cm^{-1} at the X band). For the L^2 complex the different EPR transitions are therefore spread over a broad field range. For the L^1 complex, which has even weaker exchange splittings, a similar situation is encountered. However, a nearly unsplit EPR signal is observed (fast spin relaxation limit).

Electrochemistry and Electronic Spectra. The electrochemical properties of the complexes were investigated by using cyclic (CV) and square-wave (SWV) voltammetry at stationary electrodes, linear-sweep voltammetry (LSV) at a rotating disk electrode, and spectroelectrochemistry during bulk electrolysis in combined electrochemical UV/vis cells. Formal potentials were determined in acetonitrile (0.1 M $[TBA]PF_6$) versus the ferrocenium/ferrocene couple (Fc^+/Fc) by using added ferrocene as the internal standard. For CV measurements in the thin-layer cell, $[Fe^{II}(bpy)_3](PF_6)_2$ was used as internal standard. The redox potential of the $[Fe(bpy)_3]^{3+/2+}$ couple was determined to be at +0.67 V vs Fc^+/Fc under these conditions.

Table 2. UV/Vis Spectrocopic Data of Compounds in Acetonitrile Solution

compound	λ_{max}/nm ($\epsilon_{max}/10^3$ L·mol^{-1}·cm^{-1})
$[(phenOH)Ru(bpy)_2]^{2+}$	242 (50), 291 (54), 360sh (11), 390 (12), 447sh (11), 480 (12)
$[H_2L^{1a}]^{4+}$	206sh (110), 242 (98), 289 (40), 331 (22), 394 (20), 463 (22)
$[L^{1a}Mn^{IV}_2(\mu\text{-}O)_2]^{6+}$	241 (85), 255 (79), 288 (130), 458 (30), 620sh (2.0)
$[H_3L^1]^{6+}$	206 (180), 243 (170), 289 (160), 334 (42), 391 (32), 467 (32)
$[L^1Mn^{III}]^{6+}$	208 (170), 239 (120), 287 (190), 332sh (39), 454 (40)
$[L^1Mn^{II}Mn^{II}Mn^{II}L^1]^{12+}$	210 (320), 242 (290), 288 (330), 325 (79), 387 (59), 436 (61), 457 (61)
$[(Ph)bpyRu(bpy)_2]^{2+}$	206 (60), 244 (24), 254sh (22), 287 (79), 453 (14)
$[(ArOH)bpyRu(bpy)_2]^{2+}$	244 (27), 253sh (24), 287 (78), 453 (15)
$[H_3L^2]^{6+}$	203 (260), 243 (81), 252sh (65), 287 (250), 453 (42)
$[L^2Mn^{IV}]^{7+}$	209 (260), 245 (99), 287 (270), 453 (47), 710 (8.3)
$[L^2Mn^{II}Mn^{II}Mn^{II}L^2]^{12+}$	208 (470), 246 (180), 254sh (180), 287 (500), 453 (87)

Table 3. Electrochemical Data of Compounds (Except Mn-Centered Processes)[a]

compound	$E_f(Ru^{3+}/Ru^{2+})$/V	E^{Ox} (PhOH→PhO•)/V	E_f (bpy/bpy•$^-$)/V
$[L^{1a}Mn^{IV}_2(\mu\text{-}O)_2]^{6+}$	+0.80		−1.80
$[L^1Mn^{III}]^{6+}$	+0.85		−1.80
$[L^1Mn^{II}Mn^{II}Mn^{II}L^1]^{12+}$	+0.85		−1.80
$[(ArOH)bpyRu(bpy)_2]^{2+}$	+0.85	+0.77[b]	−1.77
$[L^2Mn^{IV}]^{7+}$	+0.85	∼+0.75[c]	−1.77
$[L^2Mn^{II}Mn^{II}Mn^{II}L^2]^{12+}$	+0.85	∼+0.75[c]	−1.77

[a] Conditions: acetonitrile solution, 0.10 M tetra-*n*-butylammonium hexafluorophosphate supporting electrolyte, ferrocene (∼10^{-4} M) as internal reference, 20 °C, platinum working electrode, Ag/$AgNO_3$ (0.01 M) reference electrode. E_f represents the formal redox potential of an electrochemically reversible reaction (CV, $E_f = (E_p^{ox} + E_p^{red})/2$; SWV, E_p = peak potential); E^{Ox} represents the peak potential of an irreversible oxidative reaction. [b] Peak potential determined from CV measurement. [c] Peak potential approximated from SWV measurement.

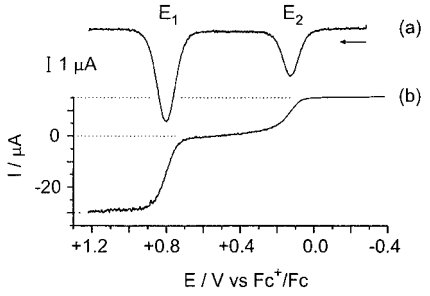

Figure 4. Square-wave voltammogram at a stationary electrode (a) and linear-sweep voltammogram at a rotating disk electrode (b) of complex $[L^{1a}Mn^{IV}_2(\mu\text{-}O)_2]^{6+}$ in acetonitrile (0.1 M TBA(PF_6)) (conditions: platinum working electrode, pulse frequency 60 Hz, pulse height 25 mV (a), rotational frequency 1000 rpm, scan rate 10 mV s^{-1}).

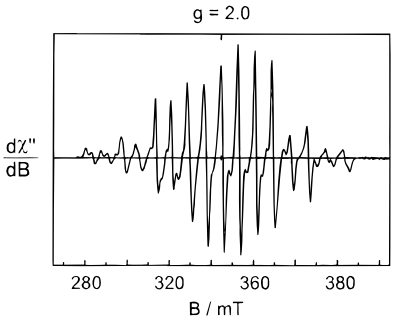

Figure 5. X-band EPR spectrum of the complex $[L^{1a}Mn^{III/IV}_2(\mu\text{-}O)_2]^{5+}$ (electrochemically generated by one-electron reduction of the parent complex $[L^{1a}Mn^{IV}_2(\mu\text{-}O)_2]^{6+}$ at −0.1 V vs Fc^+/Fc) at 30 K in an acetonitrile solution (0.1 M TBA(PF_6)) (conditions: ν = 9.64 GHz, microwave power 20 μW, modulation amplitude 5.7 G).

Square-wave and linear-sweep voltammograms recorded at stationary and rotating electrodes, respectively, of the dinuclear manganese complex $[L^{1a}Mn^{IV}_2(\mu\text{-}O)_2](PF_6)_6$ are shown in Figure 4. The redox potentials are summarized in Table 3. The reversible two-electron oxidation at $E_1 = +0.80$ V is assigned to the oxidation of the two ruthenium(II) ions to ruthenium(III), on the basis of the characteristic potential value and the observed spectrophotometric changes during bulk electrolysis: The UV/vis spectrum of the complex shows the intense ruthenium(II) → ligand charge-transfer absorption band with a maximum at 454 nm (Table 2), which disappears upon the electrochemical oxidation at +1.20 V. The second redox wave at $E_2 = +0.12$ V is assigned to the manganese-centered one-electron reduction of the $Ru^{II}_2Mn^{IV}_2$ form to the mixed-valent $Ru^{II}_2Mn^{III}Mn^{IV}$ form as indicated by the current ratio of 1:2 in the linear sweep voltammogram. During bulk electrolysis at −0.10 V, the absorption band of the Mn^{IV}_2 complex at ∼620 nm, which is assigned to a phenolate → manganese(IV) charge-transfer transition (see below), disappeared. This reduction is accompanied by a color change of the solution from green to brown. The one-electron-reduced form of the complex is EPR-active; it displays a well-resolved 16-line X-band EPR signal centered around $g = 2$ (Figure 5) characteristic of mixed-valent $Mn^{III}Mn^{IV}$ complexes. A further irreversible reduction of the mixed valent compound occurs at a peak potential of −0.71 V.

The UV/vis spectrum of the trinuclear manganese complex $[L^1Mn^{II}Mn^{II}Mn^{II}L^1]^{12+}$ shows, as expected, only very small differences from that of the free protonated ligand $[H_3L^1]^{6+}$, because it is dominated by the intense absorptions of the ruthenium-containing chromophores. In the case of the mononuclear manganese complex $[L^1Mn^{III}]^{6+}$, a significant additional absorption band is observed as a broad shoulder at about 650 nm, which is ascribed to the $^5E_g \rightarrow {}^5T_{2g}$ transition of the octahedral manganese(III) center.

The square-wave voltammograms of the mononuclear and trinuclear manganese complexes of the L^1 ligand are shown in Figure 6. The independent, reversible, ligand-centered reduction of the first of the three bpy-type ligands coordinated to each of the ruthenium(II) centers is observed at −1.80 V in both complexes as a concerted three/six-electron-transfer reaction (E_4/E_{10}). The reversible, simultaneous oxidation of the three/six equivalent ruthenium(II) ions to ruthenium(III) (E_1/E_5) on the other hand is observed at a formal potential of $E_f = +0.85$ V. Simulations of the CV waves of E_1/E_5 indicate the absence of significant differences between the individual redox potentials. Obviously, the increasing overall charge of this oxidation

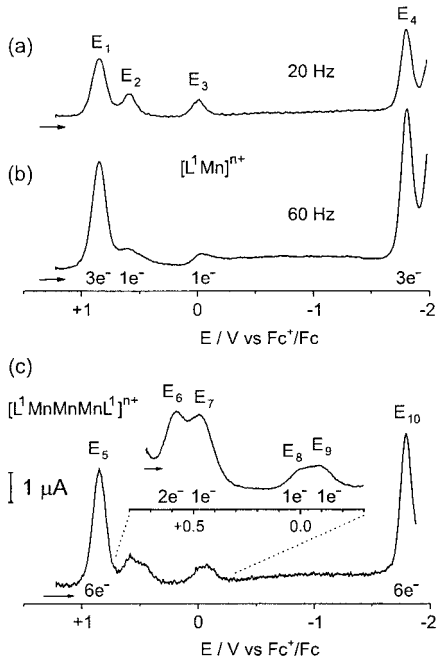

Figure 6. Square-wave voltammograms of complex $[L^1Mn^{III}]^{6+}$ in acetonitrile (0.1 M TBA(PF_6)), measured with pulse frequencies of 20 Hz (a) and 60 Hz (b) (conditions: platinum working electrode, pulse height 30 mV). Square-wave voltammogram of the complex $[L^1Mn^{II}Mn^{II}Mn^{II}L^1]^{12+}$ (b) (conditions as described in (a)). Inset: a measurement of the smaller peaks with an increased current detection sensitivity.

process displays only a negligible effect on the individual redox potential.[44] The manganese-centered redox processes (E_2; E_3; $E_6 - E_9$) are more difficult to detect, due to slow kinetics of the respective electrode reactions, but appear clearly at slower scan rates (CV) and lower pulse frequencies (SWV).

The two peaks at E_2 and E_3 in the voltammograms of the mononuclear manganese complex $[L^1Mn^{III}]^{6+}$ were identified by coulometric methods to represent a one-electron oxidation (E_2) and a one-electron reduction (E_3), respectively. They are assigned as in eq 1.

$$[L^1Mn^{IV}]^{7+} \underset{+0.59\ V}{\overset{E_2}{\rightleftharpoons}} [L^1Mn^{III}]^{6+} \underset{0.00\ V}{\overset{E_3}{\rightleftharpoons}} [L^1Mn^{II}]^{5+} \quad (1)$$

The coulometric oxidation at +0.71 V yields the one-electron-oxidized species $[L^1Mn^{IV}]^{7+}$, which shows an additional intense, broad absorption maximum at 935 nm in the UV/vis spectrum and only small differences below 700 nm as compared to the starting manganese(III) compound. Simulations of the CV waves yielded rather low values for the heterogeneous exchange rate constants of $(1-2) \times 10^{-3}$ cm·s^{-1} (E_2) and $\sim 1 \times 10^{-3}$ cm·s^{-1} (E_3) compared to at least 30×10^{-3} cm·s^{-1} for the ruthenium-centered oxidations (E_1).

Similar slow electron exchange rates were observed in the case of the trinuclear manganese(II) complex, for which several manganese-centered oxidation steps were detected (Figure 6c). In a very narrow potential range at ~0 V two reversible one-electron oxidations occur (E_8 and E_9) which are assigned to the oxidation of the two terminal manganese(II) ions. This assignment is based on the very small potential separation of 0.06 V and the spectroelectrochemical behavior. The stable $Mn^{III}Mn^{II}Mn^{III}$ species can then be oxidized in a reversible one-electron process at a formal redox potential of $E_7 = +0.47$ V, yielding the trinuclear manganese(III) species $Mn^{III}Mn^{III}Mn^{III}$. Equation 2 is consistent with all spectroscopic and electrochemical observations.

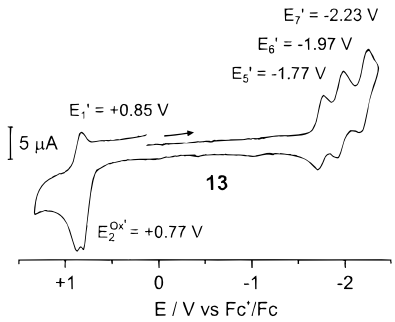

Figure 7. Cyclic voltammogram of compound **13** in acetonitrile (0.1 M TBA(PF_6)), platinum working electrode, scan rate 100 mV s^{-1}.

$$[L^1Mn^{II}Mn^{II}Mn^{II}L^1]^{12+} \underset{-0.08\ V}{\overset{E_9}{\rightleftharpoons}} [L^1Mn^{III}Mn^{II}Mn^{II}L^1]^{13+} \underset{-0.02\ V}{\overset{E_8}{\rightleftharpoons}} [L^1Mn^{III}Mn^{II}Mn^{III}L^1]^{14+} \underset{+0.47\ V}{\overset{E^7}{\rightleftharpoons}} [L^1Mn^{III}Mn^{III}Mn^{III}L^1]^{15+} \quad (2)$$

The resulting $Mn^{III}Mn^{III}Mn^{III}$ compound can electrochemically be further oxidized. The oxidation is reversible on the time scale of a square-wave voltammogram since the reverse peaks are observable ($E_6 = +0.58$ V). However, on the time scale of bulk electrolysis at +0.70 V, the oxidation is irreversible: After electrolysis the redox waves of the original compound disappeared and the signals of the respective mononuclear manganese compounds $[L^1Mn]^{n+}$ described above were observed instead. The charge equivalent of one electron was consumed during oxidation. In the UV/vis spectrum of the electrolyzed solution, the absorption band of the complex $[L^1Mn^{IV}]^{7+}$ at 935 nm appeared, and in the EPR spectrum, a new sharp six-line signal centered around $g^{eff} = 2$ was observed, which indicates the concomitant formation of a manganese(II) species. On the basis of these observations, the net reactions occurring during bulk electrolysis at +0.70 V are formulated as in eq 3.

$$[L^1Mn^{III}Mn^{III}Mn^{III}L^1]^{15+} \underset{+0.58\ V}{\overset{E_6}{\rightleftharpoons}} [L^1Mn^{IV}Mn^{III}Mn^{III}L^1]^{16+} \rightarrow 2[L^1Mn^{IV}]^{7+} + Mn^{2+} \quad (3)$$

Voltammograms of the compounds $[(ArOH)bpyRu(bpy)_2]^{2+}$ (**13**) and $[L^2Mn^{IV}]^{7+}$ are shown in Figures 7 and 8, respectively. The redox processes of the Ru(bpy)$_3$-type units were readily detected for both compounds (Ru^{3+}/Ru^{2+} at E_1' and E_1, bpy/bpy$^{\bullet-}$ at E_5' and E_5, respectively). In **13** an additional irreversible oxidation wave, which is not found in the reference compounds **11** and **12** (not shown), occurs at a peak potential of +0.77 V. This process is assigned to the irreversible oxidation of the phenol group to an unstable, probably deprotonated phenoxyl radical species.[45]

A similar irreversible process has been observed also for the manganese compound $[L^2Mn^{IV}]^{7+}$ at an approximate peak potential of $E_2^{Ox} = +0.75$ V. Again, this process is ascribed to the formation of a—now coordinated—phenoxyl radical.[23,46] Since in a standard electrochemical cell no signals of manganese-

(44) Simulations of the CV waves were perfomed using the DigiSim V 3.0 (CV) simulation program, Bioanalytical Systems, Inc., West Lafayette, IN, 1996.

(45) DeFelippis, M. R.; Murthy, C. P.; Broitman, F.; Weinraub, D.; Faraggi, M.; Klapper, M. H. *J. Phys. Chem.* **1991**, *95*, 3416−3419.

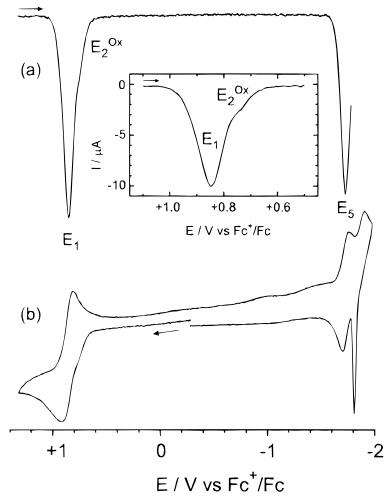

Figure 8. Square-wave voltammogram of complex $[L^2Mn^{IV}]^{7+}$ in acetonitrile (0.1 M TBA(PF_6)) (conditions: platinum working electrode, pulse frequency 60 Hz, pulse height 30 mV) (a). Inset: the positive potential range of a respective measurement with a higher resolution (pulse frequency 10 Hz, pulse height 10 mV). Cyclic voltammogram of the same solution, platinum working electrode, scan rate 100 mV s^{-1} (b).

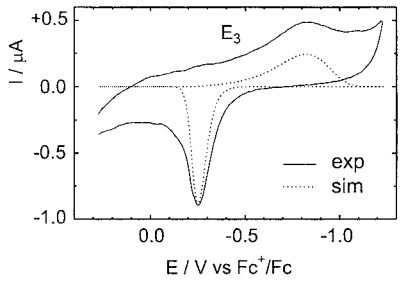

Figure 9. Cyclic voltammogram of complex $[L^2Mn^{IV}]^{7+}$ in acetonitrile (0.1 M TBA(PF_6)) in a thin-layer cell (d = 0.17 mm) (conditions: platinum net working electrode, platinum counter electrode, silver reference electrode, the $[Fe(bpy)_3]^{3+}/[Fe(bpy)_3]^{2+}$ couple was used as internal standard). Simulation of the CV waves (dotted line).

Table 4. Phenolate → Manganese(IV) CT Band

complex	λ_{max}/nm	$\epsilon_{max}/10^3$ L·mol^{-1}·cm^{-1}
$[L^{1a}Mn^{IV}{}_2(\mu\text{-}O)_2]^{6+}$	620sh	2.0
$[L^1Mn^{IV}]^{7+}$	935	4.0
$[L^2Mn^{IV}]^{7+}$	710	8.3

centered redox processes were detected for this compound, we used a thin-layer cell for measurements at very slow scan rates. Figure 9 shows the redox waves observed at a scan rate of 1 mV/s in a cell with a thickness of 0.17 mm together with the best simulation obtained assuming a one-electron process.[44] A formal redox potential of $E_3 = -0.40$ V and a standard rate constant of $k^\circ = 5 \times 10^{-6}$ cm·s^{-1} were obtained. For a satisfactory simulation of the peak shapes, a transfer coefficient as small as $\alpha = 0.2$ had to be assumed. UV/vis spectroscopy was utilized to prove that the process observed is indeed manganese-centered: The manganese(IV) starting complex shows an intense phenolate → manganese(IV) charge-transfer transition at 710 nm, which was also observed in the complexes $[L^{1a}Mn^{IV}{}_2(\mu\text{-}O)_2]^{6+}$ and $[L^1Mn^{IV}]^{7+}$ (Table 4) and in similar mononuclear phenolate−manganese(IV) complexes.[23] UV/vis spectra measured in the thin-layer cell during the CV scan show the decrease of this charge-transfer band accompanying the reductive process at ∼−0.8 V and the complete recovery of this band upon the oxidation at ∼−0.25 V, as expected for the manganese-centered redox couple $[L^2Mn^{III}]^{6+}/[L^2Mn^{IV}]^{7+}$. This was confirmed in a spectroelectrochemical experiment by performing bulk electrolysis in a standard spectroelectrochemical cell at a potential of −0.80 V with consumption of one electron per molecule, whereupon the 710 nm band disappeared completely.

A further chemically reversible one-electron reduction of the electrochemically generated $[L^2Mn^{III}]^{6+}$ complex is possible as is indicated by a very slowly proceeding bulk electrolysis at −1.50 V, but we were unable to detect any CV waves due to this process (not even using thin-layer conditions). Thus, its formal redox potential E_4 remains undetermined.

The square-wave voltammogram of the trinuclear manganese complex $[L^2Mn^{II}Mn^{II}Mn^{II}L^2]^{12+}$ is almost indistinguishable from that of the mononuclear manganese complex $[L^2Mn^{IV}]^{7+}$ shown in Figure 8. The Ru(bpy)$_3$- and phenolate-centered redox processes were again readily assigned. However, the oxidation of the manganese(II) centers was even more difficult to detect electrochemically: CV measurements with a scan rate of 1 mV·s^{-1} using thin-layer conditions show an oxidative wave at +0.2 V and a respective reductive wave at −1.1 V. This large peak separation indicates a redox process with a very low rate constant ($k^\circ < 10^{-8}$ cm·s^{-1}). Due to the influence of further irreversible oxidation processes in close proximity, the transfer coefficient and the formal redox potential could not be determined with certainty; however, −0.4 V may serve as a gross approximation. Even coulometric experiments to determine the number of electrons exchanged were unsuccessful due to the necessity of high overpotentials and the close proximity of the irreversible redox processes.

Conclusion

A series of new N- and O-donating ligands containing covalently attached Ru(bpy)$_3$-type moieties was designed and synthesized. With these multidentate ligand systems several heterooligonuclear complexes containing one, two, or three manganese ions and up to six tris(2,2′-bipyridyl)ruthenium(II) groups were obtained in a synthetically stepwise fashion by which the nuclearity of the complexes is controlled by the reaction conditions employed. The tris(bipyridyl)ruthenium(II) units were chosen because they are able to undergo light-energy-induced charge separation and are therefore considered to be a model of the reaction center P680 in photosystem II. The linkage to the manganese ions was achieved by choosing different spacer groups. In the case of the ligand $[L^2]^{3-}$, electron-rich phenolates were used, stabilizing phenoxyl radical species. In a mononuclear manganese(IV) complex of this ligand, electrochemical one-electron oxidation of the phenolate group to a phenoxyl radical was observed.

In general the manganese centers in these complexes have been shown to exist in the oxidation states II, III, and IV. They can undergo metal-centered reversible one-electron-transfer steps. In several cases very slow heterogeneous electron-transfer processes have been observed electrochemically. The transfer rates depend on the length of the spacer separating the manganese ions from the electrode surface. The longer spacer in the bulky L^2 ligand system gives rise to particularly slow electron-exchange kinetics; thin-layer electrochemical methods have been successfully utilized to study these reactions.

The compounds presented here serve as structural and functional models for the donor site of photosystem II. They model the light-driven oxidation of the reaction center P680

(46) Burdinski, D.; Wieghardt, K.; Steenken, S. *J. Am. Chem. Soc.* **1999**, *121*, 10781−10787.

and its subsequent reduction by an enzyme-bound redox-active tyrosine. In this reaction a tyrosyl radical is formed as an intermediate, which then repetitively oxidizes the nearby manganese cluster, where, finally, the four-electron oxidation of two water molecules to dioxygen occurs. Similar reactions occur in the model complexes described here upon photochemical excitation of the ruthenium-containing part of the compounds. These laser-flash photolysis experiments are described in a subsequent paper.[46]

Experimental Section

General Methods. Nuclear magnetic resonance spectra (^{1}H NMR and ^{13}C NMR) were obtained on a Bruker spectrometer ARX 250, DRX 400, or DRX 500. Infrared spectra were recorded on a Perkin-Elmer 2000 FT-IR instrument. Electron impact (EI) mass spectra were measured on a Finnigan MAT 8200 spectrometer. Electrospray (ESI) mass spectra were obtained on a Finnigan MAT 95 or a Hewlet-Packard 5989 instrument using sample solutions in methanol or acetonitrile. Elemental analyses were determined by the Mikroanalytisches Labor Kolbe, Mülheim an der Ruhr, Germany; satisfactory elemental analyses were obtained for all compounds. Thin-layer chromatography (TLC) was performed on Merck Kieselgel 60 F_{254} precoated silica gel plates or on Merck Aluminum Oxide 60 F_{254} precoated basic alumina plates. Spots were visualized by irradiation with ultraviolet light (254 and 366 nm) and/or by dipping the plate in a freshly prepared aqueous solution of $[NH_4]Fe(SO_4)_2 \cdot 6H_2O$; 2,2′-bipyridyls and 1,10-phenathrolines produce various colors with Fe^{2+}, mostly red to purple. The following solvent mixtures were used for TLC of complexes on silica gel: (a) KNO_3 (saturated solution in H_2O)/H_2O/CH_3CN (1:4:5), (b) KNO_3 (saturated solution in H_2O)/H_2O/CH_3CN/NH_3 (25% solution in H_2O) (80:320:400:7), (c) KNO_3 (saturated solution in H_2O)/H_2O/CH_3CN (1:14:5). Column chromatography was performed on deactivated basic alumina (ICN Alumina B−Super I, ICN Biochemicals, activity grade III; $Al^{III}_2O_3$) or Sephadex LH20 (Pharmacia Biotech; column 200 cm × 3 cm, eluent methanol, light protection!). Preparative gas chromatography (GC) was performed on a Gerstel AMPG-60 instrument equipped with a Volasphere A4 column (100−120 mesh, 20 mm × 500 mm, coated with 20% SE-30) at constant temperature (220 °C). All reactions with ruthenium-containing complexes were performed under exclusion of light.

Materials. 4,4′-Dimethyl-2,2′-bipyridyl, 2,2′-bipyridyl (bpy), 1,2-dibromoethane, diisopropylamine (redistilled 99.5%), *p*-toluenesulfonic acid monohydrate, and sodium methoxide were purchased from Aldrich. Ammonium hexafluorophosphate (Fluka), *n*-butyllithium (1.6 M solution in hexane; Chemetall), tetra-*n*-butylammonium chloride hydrate (Fluka), tetra-*n*-butylammonium fluoride (1 M solution in THF; ABCR-Chemicals), ruthenium trichloride (Heraeus), and sodium borohydride (Fluka) were also used as received.

Tetrahydrofuran (THF) was distilled from lithium aluminum hydride ($LiAlH_4$) prior to use. Acetonitrile was dried over calcium chloride and distilled over molecular sieves (3 Å). Methanol was also distilled over molecular sieves (3 Å). Toluene was dried over calcium chloride and distilled from sodium.

1,4,7-Triazacyclononane (tacn),[47,48] *cis*-$[(bpy)_2RuCl_2] \cdot 2H_2O$,[49] and 4-((*tert*-butyldimethylsilyl)oxy)-3-methoxybenzyl bromide[50] were prepared according to published procedures. 4-Hydroxy-1,10-phenanthroline (phenOH) was prepared by the method reported by Snyder et al.[51] and further purified by Soxhlet extraction with toluene.

1,4,7-Triazatricyclo[5.2.1.0^{4,10}]decane (1). 1,4,7-Triazacyclononane (80.0 g, 620 mmol), triethyl orthoformate (96.5 g, 651 mmol), and *p*-toluenesulfonic acid monohydrate (2.95 g, 15.5 mmol) were heated in a short-path distillation apparatus on an oil bath at 150 °C for several hours until the calculated amount of ethanol (109 mL) had evolved. The pure product was obtained as a colorless oil by vacuum distillation. Yield: 76.0 g, (88%). Bp: 60−63 °C (2×10^{-2} mbar). ^{1}H NMR (400 MHz, $CDCl_3$, ppm): δ 4.51 (s, 1H), 2.57 (m, 6H), 2.31 (m, 6H). ^{13}C NMR (100 MHz, $CDCl_3$, ppm): δ 103.2, 51.0. EI-MS: *m*/*z* 139 (M^+), 97, 83, 70, 56, 42.

1,2-Bis(4-methyl-1,4,7-triazacyclononyl)ethane, Me$_2$dtne (3). To a solution of **1** (30.0 g, 220 mmol) in acetonitrile (100 mL) was added 1,2-dibromoethane (20.3 g, 110 mmol) with stirring. The solution was allowed to stand at ambient temperature in a sealed reaction vessel for about one week. The yellow, hygroscopic, crystalline precipitate formed was collected by filtration, washed rapidly with diethyl ether, and dried over P_4O_{10} to yield colorless 1,2-bis(4,7-diaza-1-diazoniatricyclo-[5.2.1.0^{4,10}]decyl)ethane dibromide (**2**) (48.8 g, 95% yield).

To a suspension of **2** (20.0 g, 42.9 mmol) in methanol (700 mL) in a 6 L round-bottom flask equipped with a reflux condenser was added sodium borohydride (16.2 g, 429 mmol) within 5 min (*Caution! This is a very exothermic reaction*). When the reaction had calmed down, the mixture was transferred to a 1 L round-bottom flask and refluxed for 30 min, after which time the solvent was removed by rotary evaporation. The remaining white mass was suspended in concentrated hydrochloric acid (150 mL) and refluxed for 90 min. After the suspension was cooled in an ice bath, the white precipitate was removed by suction filtration and washed with ice-cold concentrated hydrochloric acid. The combined filtrates were rotary evaporated to dryness, and the residue was resuspended in 3 M hydrochloric acid (20 mL). After filtration and washing of the residue with ice-cold 3 M hydrochloric acid (2 × 7 mL), the combined filtrates were refluxed for a further 60 min and cooled in an ice bath. The pH was adjusted to 12 by addition of solid sodium hydroxide. The precipitate formed was removed by suction filtration, the pH of the filtrate adjusted to 13−14, and the colorless solution extracted with *n*-pentane (3 × 250 mL). Then the pH of the aqueous phase was adjusted to >14 until a second phase appeared. This was extracted with *n*-pentane (4 × 250 mL), and the combined extracts were dried over Na_2SO_4. After filtration and removal of the solvent in vacuo, a colorless oil of crude **3** (∼8 g) remained. This material was vacuum distilled in a concentric-tube column (System Fischer, 300 mm), giving a colorless oil that solidified at room temperature within a few hours. Yield: ∼4 g (30%). Bp: 130 °C (0.05 Torr). ^{1}H NMR (400 MHz, D_2O, ppm): δ 2.62 (s, 4H), 2.53 (s, br, 20H), 2.45 (s, br, 4H), 2.22 (s, 6H). ^{13}C NMR (100 MHz, D_2O, ppm): δ 54.5, 53.7, 52.8, 51.8, 51.1, 45.2, 44.9 (CH_3), 44.7. EI-MS: *m*/*z* 312 (M^+), 170, 156. FT-IR (KBr, cm^{-1}): 2944, 2921, 2851, 2814, 2790, 1583, 1460, 1401, 1371, 1273, 812, 628, 590.

4-Methyl-4′-(phenethyl)-2,2′-bipyridyl ((Ph)bpy). In an argon-flushed round-bottom flask, 1.6 M *n*-butyllithium in *n*-hexane (13.6 mL, 21.7 mmol) was added to a stirred solution of diisopropylamine (3.22 mL, 23 mmol) in THF (20 mL). After 10 min of stirring, the mixture was cooled to −78 °C, and a solution of Me_2bpy (4.00 g, 21.7 mmol) in THF (200 mL) was added within 30 min. The dark brown reaction mixture was stirred for 90 min, then a solution of benzyl chloride (2.5 mL, 21.7 mmol) in THF (20 mL) was added slowly, and the resulting solution was stirred for an additional hour. It was then allowed to warm to room temperature and stirred overnight. The reaction was quenched by the addition of water (50 mL) followed by extraction with ether (1 × 400 mL) and CH_2Cl_2 (2 × 100 mL). The combined organic layers were dried (Na_2SO_4) and evaporated under reduced pressure, yielding a yellow solid. This was redissolved in CH_2Cl_2, adsorbed on basic alumina (10 g), and chromatographed ($Al^{III}_2O_3$, pentane/ether 10:1, $R_f \approx 0.05$) to give a mixture of mono- and unsubstituted Me_2bpy, which could not be separated by column chromatography, but by preparative GC. The product is a white solid. Yield: 0.82 g (14%). Mp: 80 °C. ^{1}H NMR (400 MHz, $CDCl_3$, ppm): δ 8.52 (d, J = 5 Hz, 2H), 8.27 (s, 1H), 8.22 (s, 1H), 7.27 (t, J = 7 Hz, 2H), 7.18 (t, J = 7 Hz, 1H), 7.17 (d, J = 7 Hz, 2H), 7.11 (d, J = 4.8 Hz, 1H), 7.06 (d, J = 4.8 Hz, 1H), 2.98 (s, 4H), 2.41 (s, 3H). ^{13}C NMR (100 MHz, $CDCl_3$, ppm): δ 156.2, 156.0, 151.6, 149.0, 148.9, 148.1, 140.9, 128.5, 128.4, 126.2, 124.6, 123.9, 122.0, 121.2, 37.4, 36.7, 21.1. EI-MS: *m*/*z* 273 ($[M - H]^+$), 197, 170, 91.

(47) Wieghardt, K.; Schmidt, W.; Nuber, B.; Weiss, J. *Chem. Ber.* **1979**, *112*, 2220−2230.
(48) Atkins, T. J.; Richman, J. E.; Oettle, W. F. *Org. Synth.* **1978**, *58*, 86−96.
(49) Lay, P. A.; Sargeson, A. M.; Taube, H. *Inorg. Synth.* **1986**, *24*, 291−299.
(50) Singh, S. B.; Pettit, G. R. *Synth. Commun.* **1987**, *17*, 877−892.
(51) Snyder, H. R.; Freier, H. E. *J. Am. Chem. Soc.* **1946**, *68*, 1320−1322.

4-(2-(4-((*tert*-Butyldimethylsilyl)oxy)-3-methoxyphenyl)ethyl)-4′-methyl-2,2′-bipyridyl (4). A solution of lithium diisopropylamide (LDA) in THF (50 mL) was prepared by the reaction of diisopropylamine (12.1 mL, 86 mmol) with 1.6 M *n*-butyllithium in *n*-hexane (53.8 mL, 86 mmol). After this solution was cooled to −78 °C, a solution of Me_2bpy (15.0 g, 81.4 mmol) in THF (650 mL) was added dropwise within 60 min. The dark brown mixture was stirred at −78 °C for an additional 90 min. Then 4-((*tert*-butyldimethylsilyl)oxy)-3-methoxybenzyl bromide (27.0 g, 81.4 mmol) dissolved in THF (100 mL) was added slowly (30 min), whereupon the color changed to green and finally to yellow. After 60 min the solution was allowed to warm to room temperature and stirred for 2 h. The reaction was quenched by addition of water (250 mL) followed by extraction with ether (1 × 1000 mL) and CH_2Cl_2 (2 × 250 mL). The combined organic layers were dried (Na_2SO_4), and the solvents were evaporated under reduced pressure, yielding a yellow-brown oil. Traces of solvent were removed in vacuo (3×10^{-3} mbar) for several hours. The remaining semisolid mass was suspended in 40 mL of petroleum ether (bp 60−80 °C) and stored overnight at 4 °C. The white precipitate formed was removed by suction filtration, washed twice with petroleum ether and three times with *n*-pentane, and discarded (the isolated solid (∼6 g) consists predominantly of Me_2bpy). The combined filtrates were rotary evaporated; the resulting yellow-brown oil was adsorbed on basic alumina and chromatographed ($Al^{III}_2O_3$, pentane/ether 10:1, $R_f \approx 0.05$). The product was a colorless oil that solidified at room temperature within a few hours. Yield: 11.0 g (31%). ^{1}H NMR (400 MHz, $CDCl_3$): δ 8.50 (d, $J = 4.5$ Hz, 1H), 8.49 (d, $J = 4.5$ Hz, 1H), 8.23 (s, 1H), 8.20 (s, 1H), 7.08 (d, $J = 4.5$ Hz, 1H), 7.00 (d, $J = 4.5$ Hz, 1H), 6.72 (d, $J = 8.5$ Hz, 1H), 6.59 (m, 2H), 3.70 (s, 3H), 2.90 (m, 4H), 2.39 (s, 3H), 0.96 (s, 9H), 0.10 (s, 6H). ^{13}C NMR (100 MHz, $CDCl_3$, ppm): δ 156.1, 155.9, 151.6, 150.6, 148.9, 148.8, 148.0, 143.2, 134.3, 124.5, 124.0, 121.9, 121.2, 120.7, 120.4, 112.5, 55.3, 37.6, 36.4, 25.7, 21.1, 18.3, −4.8. EI-MS: *m*/*z* 434 (M^+), 419, 377, 198.

4-(2-(4-Hydroxy-3-methoxyphenyl)ethyl)-4′-methyl-2,2′-bipyridyl ((ArOH)bpy). A solution of compound **4** (10.0 g, 23.0 mmol) in THF (70 mL) was treated with a 1.0 M solution of tetrabutylammonium fluoride in THF (25 mL, 25 mmol) and stirred for 30 min. Water (30 mL) was added to the light yellow reaction mixture, and it was extracted with ether (400 mL). The colorless organic phase was washed with water (2 × 30 mL), dried (Na_2SO_4), and rotary evaporated. The remaining semisolid mass was refluxed with *n*-hexane (3 × 200 mL) and the hexane decanted hot. The white crystalline product precipitated from the combined hexane phases. It was collected by filtration, washed with *n*-hexane and *n*-pentane, and air-dried. Yield: 6.8 g (92%). ^{1}H NMR (250 MHz, $CDCl_3$, ppm): δ 8.51 (d, $J = 5.0$ Hz, 2H), 8.25 (s, 1H), 8.20 (s, 1H), 7.10 (d, $J = 5.0$ Hz, 1H), 7.03 (d, $J = 5.0$ Hz, 1H), 6.79 (d, $J = 7.8$ Hz, 1H), 6.63 (d, $J = 7.8$ Hz, 1H), 6.60 (s, 1H), 6.10 (s, br, 1H), 3.75 (s, 3H), 2.89 (m, 4H), 2.39 (s, 3H). ^{13}C NMR (62.9 MHz, $CDCl_3$, ppm): δ 156.1, 155.9, 151.7, 148.9, 148.8, 148.2, 146.5, 144.0, 132.7, 124.6, 124.0, 122.1, 121.3, 120.8, 114.4, 111.1, 55.7, 37.7, 36.3, 21.1. EI-MS: *m*/*z* 320 (M^+), 184, 198.

1,2-Bis(4-((4-hydroxy-1,10-phenanthrolin-3-yl)methyl)-7-methyl-1,4,7-triazacyclononyl)ethane (Me_2dtne(CH_2(phenOH))$_2$) (5). Me_2-dtne (1.65 g, 5.28 mmol) was treated with a methanol solution (10 mL) of paraformaldehyde (350 mg, 11.6 mmol). After the mixture was stirred overnight at room temperature, the methanol was evaporated under reduced pressure. The oily residue was dissolved in toluene (50 mL) and added to an argon-flushed toluene suspension (400 mL) of phenOH (2.28 g, 11.6 mmol). The mixture was refluxed for 48 h in an argon atmosphere, whereupon the phenOH dissolved completely before a slimy, brown precipitate formed within a few hours. It was decanted hot (!). After the mixture was allowed to stand overnight at 4 °C, a crystalline precipitate formed which was filtered off, washed with toluene, ether, and *n*-pentane, and air-dried, yielding a light yellow solid of sufficient purity (80−90%) for preparative purposes. Yield: 2.5 g (65%). An analytically pure sample was obtained as the second band by column chromatography ($Al_2^{III}O_3$) using an ether/methanol gradient (4:1−0:1) as eluent. The pure sample was a light yellow powder. ^{1}H NMR (250 MHz, $CDCl_3$, ppm): δ 8.85 (d, br, 2H), 8.40 (d, $J = 8.9$ Hz, 2H), 8.28 (s, 2H), 8.19 (d, br, $J = 8$ Hz, 2H), 7.59−7.51 (m, 4H), 3.83 (s, br, 4H), 3.0−2.6 (m, br, 24H), 2.59 (s, 4H), 2.33 (s, 6H). ESI-MS (positive ion, CH_3OH): *m*/*z* 729 ($[M + H]^+$), 365 ($[M + 2H]^{2+}$).

1,4,7-Tris((4-hydroxy-1,10-phenanthrolin-3-yl)methyl)-1,4,7-triazacyclononane (tacn(CH_2(phenOH))$_3$) (6). A solution of tacn (0.57 g, 4.4 mmol) and paraformaldehyde (0.41 g, 14 mmol) in methanol (30 mL) was stirred overnight at room temperature and rotary evaporated under reduced pressure. The solution of the oily residue in toluene (50 mL) was added to an argon-flushed suspension of phenOH (3.00 g, 15.3 mmol) in toluene (400 mL) and refluxed for 48 h. The phenOH dissolved completely before a fine, light precipitate formed, which was filtered off hot (!), washed with toluene, ether, and *n*-pentane, and air-dried, yielding a light beige powder of sufficient purity (70−80%) for preparative purposes. Yield: 1.8 g (54%). To obtain an analytical pure sample, the crude product was chromatographed ($Al^{III}_2O_3$) using a CH_2Cl_2/CH_3OH gradient (5:0−5:1) as eluent. ^{1}H NMR (400 MHz, CD_3OD): δ 8.83 (dd, $J = 4.3$ Hz, $J' = 1.6$ Hz, 3H), 8.37 (s, 3H), 8.23 (d, $J = 9.0$ Hz, 3H), 8.15 (dd, $J = 8.2$ Hz, $J' = 1.6$ Hz, 3H), 7.53 (dd, $J = 8.2$ Hz, $J' = 4.3$ Hz, 3H), 7.49 (d, $J = 9.0$ Hz, 3H), 3.90 (s, 6H), 2.92 (s, 12H). ^{13}C NMR (100 MHz, CD_3OD, ppm): δ 177.7, 150.0, 143.3 (br), 141.9, 140.6 (br), 136.9, 130.0, 124.9, 124.5, 123.4, 123.3, 119.9 (br), 55.0, 52.6. ESI-MS (positive ion, CH_3OH): *m*/*z* 754 ($(M + H)^+$).

1,4,7-Tris(2-hydroxy-3-methoxy-5-(2-(4′-methyl-2,2′-bipyridyl-4-yl)ethyl)benzyl)-1,4,7-triazacyclononane (tacn(CH_2(ArOH)bpy)$_3$) (7). An argon-flushed solution of tacn (100 mg, 0.77 mmol) and paraformaldehyde (78 mg, 2.6 mmol) in methanol was refluxed for 30 min. After addition of (ArOH)bpy (1.00 g, 3.12 mmol), the reaction mixture was refluxed for 72 h in an argon atmosphere and rotary evaporated to a viscous yellow oil, which was directly used in the next step of the synthesis. An analytically pure sample was obtained in a very low yield by dissolving the crude product in a minimum amount of THF and dropping it into an excess of dry ether. The precipitated product was filtered off, washed with ether, and air-dried, yielding a light beige powder. ^{1}H NMR (400 MHz, $CDCl_3$): δ 8.52−8.46 (m, 6H), 8.23 (s, 3H), 8.20 (s, 3H), 7.09 (d, br, $J = 4$ Hz, 3H), 7.03 (d, br, $J = 4$ Hz, 3H), 6.59 (d, $J = 1.4$ Hz, 3H), 6.38 (d, $J = 1.4$ Hz, 3H), 3.80 (s, 9H), 3.76 (d, $J = 4$ Hz, 3H), 3.65 (s, br, 3H), 2.94−2.88 (m, 12H), 2.86−2.80 (m, 12H), 2.40 (s, 9H). ESI-MS (positive ion, CH_3OH): *m*/*z* 1126 ($[M + H]^+$).

[Me_2bpyRu(bpy)$_2$](PF_6)$_2$ (11). An argon-flushed solution of Me_2-bpy (0.37 g, 2.0 mmol) and *cis*-[(bpy)$_2$$RuCl_2$]·$2H_2O$ in ethanol/water (50:50, 40 mL) was refluxed for 5 h. After the mixture was cooled to room temperature and filtration, the crude product was precipitated by addition of a saturated aqueous solution of NH_4PF_6 (0.8 g), isolated by filtration, washed with water, ethanol, and ether, and recrystallized from ethanol (96%)/acetone (70:30). The crystalline product was filtered, washed with ethanol and ether, and air-dried, yielding a bright orange powder. Yield: 1.33 g (75%). R_f(a) = 0.85. ^{1}H NMR (250 MHz, CD_3-CN, ppm): δ 8.51 (d, $J = 8.1$ Hz, 4H), 8.39 (s, 2H), 8.05 (t, $J = 7.6$ Hz, 4H), 7.76 (m, 4H), 7.56 (d, $J = 5.7$ Hz, 2H), 7.42 (t, $J = 7$ Hz, 2H), 7.40 (t, $J = 7$ Hz, 2H), 7.24 (d, $J = 5.7$ Hz, 2H), 2.52 (s, 6H). ESI-MS (positive ion, CH_3CN): *m*/*z* 743 ($[M - (PF_6)]^+$), 299 ($[M - 2(PF_6)]^{2+}$). UV/vis (CH_3CN): λ_{max}/nm (ϵ/10^3 L·mol^{-1}·cm^{-1}) 206 (57), 245 (24), 254sh (22), 287 (85), 454 (15).

[(Ph)bpyRu(bpy)$_2$](PF_6)$_2$ (12). An argon-flushed solution of (Ph)-bpy (0.41 g, 1.5 mmol) and *cis*-[(bpy)$_2$$RuCl_2$]·$2H_2O$ (0.78 g, 1.5 mmol) in ethanol/water (50:50, 40 mL) was refluxed for 5 h, cooled to room temperature, and filtered. A saturated aqueous solution of NH_4PF_6 (0.8 g) was added, and the precipitate formed was collected by filtration and washed with water, ethanol, and ether. The crude product was recrystallized from ethanol (96%)/acetone (70:30), washed with ethanol and ether, and air-dried, yielding a bright orange powder. Yield: 1.33 g (75%). R_f(a) = 0.80, R_f(c) = 0.38. ^{1}H NMR (250 MHz, CD_3CN, ppm): δ 8.51 (d, $J = 8.2$ Hz, 4H), 8.34 (d, br, $J = 5$ Hz, 2H), 8.10−8.02 (m, 4H), 7.75 (d, $J = 5.6$ Hz, 3H), 7.71 (d, $J = 5.4$ Hz, 1H), 7.55 (d, $J = 5.8$ Hz, 2H), 7.47−7.37 (m, 4H), 7.27−7.12 (m, 7H), 3.15−2.96 (m, 4H), 2.54 (s, 3H). ESI-MS (positive ion, CH_3CN): *m*/*z* 833 ($[M - (PF_6)]^+$), 344 ($[M - 2(PF_6)]^{2+}$. UV/vis (CH_3CN): λ_{max}/nm (ϵ/10^3 L·mol^{-1}·cm^{-1}) 206 (60), 244 (24), 254sh (22), 287 (79), 453 (14).

[(ArOH)bpyRu(bpy)$_2$](PF_6)$_2$ (13). (ArOH)bpy (0.48 g, 1.5 mmol) and *cis*-[(bpy)$_2$$RuCl_2$]·$2H_2O$ (0.78 g, 1.5 mmol) were dissolved in

ethanol/water (50:50, 40 mL), refluxed for 5 h in an argon atmosphere, cooled to room temperature, and filtered. The crude product was precipitated by addition of a saturated aqueous solution of NH_4PF_6 (0.8 g), isolated by filtration, washed with water, ethanol, and ether, and chromatographed (silica gel, KNO_3 (saturated solution in H_2O)/H_2O/CH_3CN/CH_3OH (1:4:5:10)). The solvents of the combined pure fractions were removed by rotary evaporation, and the residue was redissolved in water and a small amount of acetone. After addition of an excess of a saturated aqueous solution of NH_4PF_6, the pure product crystallized upon slow evaporation. It was isolated by filtration, washed with water, ethanol, and ether, and air-dried, yielding a bright orange powder. Yield: 0.62 g (40%). R_f(a) = 0.80, R_f(c) = 0.35. ^{1}H NMR (250 MHz, CD_3CN, ppm): δ 8.49 (d, J = 8.2 Hz, 4H), 8.31 (s,1H), 8.27 (s, 1H), 8.09−8.00 (m, 4H), 7.72 (d, J = 5.5 Hz, 3H), 7.66, (d, J = 5.2 Hz, 1H), 7.52 (d, J = 5.8 Hz, 2H), 7.41 (t, J = 7 Hz, 2H), 7.38 (t, J = 7 Hz, 2H), 7.22 (d, br, J = 5.8 Hz, 1H), 7.16 (dd, J = 5.8 Hz, J′=1.6 Hz, 1H), 6.79 (d, J = 1.8 Hz, 1H), 6.65 (d, J = 8.0 Hz, 1H), 6.56 (dd, J = 8.0 Hz, J′=1.8 Hz, 1H), 6.36 (s, br, 1H), 3.75 (s, 3H), 3.08 (t, br, J = 7 Hz, 2H), 2.91 (t, br, J = 7 Hz, 2H), 2.58 (s, 3H). ESI-MS (positive ion, CH_3CN): m/z 879 ($[M - (PF_6)]^+$), 367 ($[M - 2(PF_6)]^{2+}$). UV/vis (CH_3CN): λ_{max}/nm ($\epsilon/10^3$ L·mol^{-1}·cm^{-1}) 244 (27), 253sh (24), 287 (78), 453 (15).

[(phenOH)Ru(bpy)$_2$](PF$_6$)$_2$ (14). A solution of phenOH (0.30 g, 1.5 mmol) and *cis*-[(bpy)$_2$RuCl$_2$]·2H$_2$O (0.78 g, 1.5 mmol) in ethanol/water (50:50, 30 mL) was refluxed for 5 h in an argon atmosphere. After removal of the ethanol in vacuo, more water (15 mL) was added and the crude product precipitated by the addition of a few drops of concentrated aqueous hexafluorophosphoric acid. It was collected by filtration, washed with water and ether, and redissolved in acetone (40 mL). Then a concentrated solution of tetra-*n*-butylammonium chloride hydrate in acetone was added, whereupon the chloride salt precipitated. It was filtered off, washed with acetone and ether, redissolved in water, precipitated by the addition of concentrated HPF_6, and isolated as described above. The hexafluorophosphate salt was recrystallized once from hot ethanol/water (50:50) and air-dried, yielding an orange powder. Yield: 0.8 g (60%). R_f(a) = 0.50. ^{1}H NMR (250 MHz, CD_3CN, ppm): δ 8.56−8.46 (m, 5H), 8.39 (d, J = 9.0 Hz, 1H), 8.09−8.00 (m, 4H), 7.97 (td, J = 7.9 Hz, J′=1.4 Hz, 2H), 7.85 (t, br, J = 6.2 Hz, 2H), 7.69−7.56 (m, 4H), 7.45−7.39 (m, 2H), 7.26−7.19 (m, 2H), 7.08 (d, J = 6.2 Hz, 1H). ESI-MS (positive ion, CH_3CN): m/z 755 ($[M - (PF_6)]^+$), 305 ($[M - 2(PF_6)]^{2+}$), 609 ($[M - H(PF_6)_2]^+$). UV/vis (CH_3CN): λ_{max}/nm ($\epsilon/10^3$ L·mol^{-1}·cm^{-1}) 242 (50), 291 (54), 360sh (11), 390 (12), 447sh (11), 480 (12). Anal. Calcd for $C_{32}H_{24}N_6O_1Ru_1(PF_6)_2$: C, 42.73; H, 2.69; N, 9.34; Ru, 11.24. Found: C, 42.40; H, 2.79; N, 9.20; Ru, 10.98.

[Me$_2$dtne(CH$_2$(phenOH)Ru(bpy)$_2$)$_2$](PF$_6$)$_4$, [H$_2$L^{1a}](PF$_6$)$_4$. Me$_2$-dtne(CH$_2$(phenOH))$_2$ (0.48 g, 0.66 mmol) and *cis*-[(bpy)$_2$RuCl$_2$]·2H$_2$O (1.04 g, 2.0 mmol) were dissolved in methanol (60 mL) and refluxed in an argon atmosphere for 48 h. After removal of the solvent by rotary evaporation, the red residue was taken up in methanol (2−3 mL) and stored overnight at 4 °C. The deep-red solution was filtered and chromatographed in portions (Sephadex LH20). The first red band was collected and evaporated to dryness and the product precipitated from water by addition of a saturated aqueous solution of NH_4PF_6. Filtration, washing with water and ether, and drying in air yielded the product as a red-brown powder. Yield: 0.50 g (36%). R_f(b) = 0.50. ^{1}H NMR: In CD_3CN and in CD_3OD only two broad multiplets (δ 8.6−6.8, 4.0−1.5) could be detected. ESI-MS (positive ion, CH_3CN): m/z 311 ($[CH_2$-(phenO)Ru(bpy)$_2]^{2+}$). UV/vis (CH_3CN): λ_{max}/nm ($\epsilon/10^3$ L·mol^{-1}·cm^{-1}) 206sh (110), 242 (98), 289 (40), 331 (22), 394 (20), 463 (22). Anal. Calcd for $C_{82}H_{84}N_{18}O_2Ru_2(PF_6)_4$: C, 46.12; H, 3.96; N, 11.81; Ru, 9.46. Found: C, 45.92; H, 3.98; N, 11.65; Ru, 9.31.

[tacn(CH$_2$(phenOH)Ru(bpy)$_2$)$_3$](PF$_6$)$_6$, [H$_3$L^1](PF$_6$)$_6$. A solution of tacn(CH$_2$(phenOH))$_3$ (0.43 g, 0.57 mmol) and *cis*-[(bpy)$_2$RuCl$_2$]·2H$_2$O (1.19 g, 2.29 mmol) in methanol (60 mL) was refluxed for 72 h in an argon atmosphere and treated further as described above. The product obtained after chromatography and precipitation from water was a red-brown powder. Yield: 0.40 g (25%). R_f(a) = 0.30; R_f(b) = 0.64. ^{1}H NMR (400 MHz, CD_3OD/CD_3CN (3:1), ppm): δ 8.93 (s, br, 3H), 8.60−8.40 (m, 12H), 8.40−8.20 (m, 6H), 8.20−8.10 (m, br, 3H), 8.10−7.80 (m, 21H), 7.75−7.63 (m, 3H), 7.61−7.45 (m, 9H), 7.45−7.38 (m, 3H), 7.38−7.25 (m, 6H), 7.25−7.15 (m, 3H), 4.11 (d, br, J = 13 Hz, 3H), 3.93 (d, br, J = 13 Hz, 3H), 3.10−2.65 (m, br, 12H). ESI-MS (positive ion, CH_3CN): m/z 311 ($[CH_2$(phenO)Ru(bpy)$_2]^{2+}$). UV/vis (CH_3CN): λ_{max}/nm ($\epsilon/10^3$ L·mol^{-1}·cm^{-1}) 206 (180), 243 (170), 289 (160), 334 (42), 391 (32), 467 (32). Anal. Calcd for $C_{105}H_{87}N_{21}O_3Ru_3$-$(PF_6)_6$: C, 44.04; H, 3.06; N, 10.27; Ru, 10.59. Found: C, 43.41; H, 3.16; N, 9.98; Ru, 10.21.

[tacn(CH$_2$(ArOH)bpyRu(bpy)$_2$)$_3$](PF$_6$)$_6$, [H$_3$L^2](PF$_6$)$_6$. The crude tacn(CH$_2$(ArOH)bpy)$_3$ (<0.8 mmol) and *cis*-[(bpy)$_2$RuCl$_2$]·2H$_2$O (1.30 g, 2.5 mmol) were dissolved in methanol (30 mL), refluxed for 15 h in an argon atmosphere, and treated further as described above. The product was a light orange-brown powder. Yield: 0.90 g (36%). R_f(a) = 0.40. ^{1}H NMR (400 MHz, CD_3OD, ppm): δ 8.70 (m, br, 18H), 8.11 (s, br, 12H), 7.80 (s, br, 12H), 7.60 (s, br, 6H), 7.49 (s, br, 12H), 7.34 (s, br, 6H), 6.86 (s, br, 3H), 6.80 (s, br, 3H), 8.82 (s, br, 6H), 3.75 (s, br, 9H), 3.16 (s, br, 6H), 3.01 (s, br, 6H), 2.76 (s, br, 9H), 2.58 (s, br, 12H). ESI-MS (positive ion, CH_3CN): m/z 891 ($[[CH_2$(ArO)bpyRu-(bpy)$_2](PF_6)]^+$, 373 ($[CH_2$(ArO)bpyRu(bpy)$_2]^{2+}$). UV/vis (CH_3CN): λ_{max}/nm ($\epsilon/10^3$ L·mol^{-1}·cm^{-1}) 203 (260), 243 (81), 252sh (65), 287 (250), 453 (42). Anal. Calcd for $C_{129}H_{123}N_{21}O_6Ru_3(PF_6)_6$: C, 47.87; H, 3.83; N, 9.09; Ru, 9.37. Found: C, 46.86; H, 3.99; N, 8.85; Ru, 9.52.

[L^{1a}Mn^{IV}Mn^{IV}(μ-O)$_2$](PF$_6$)$_6$. To the deep red solution of [H$_2$L^{1a}]-(PF$_6$)$_4$ (0.42 g, 0.20 mmol) in ethanol/acetone (50:50, 40 mL) was added [Mn$_3$(μ_3-O)(μ-CH$_3$CO$_2$)$_6$(H$_2$O)$_3$](CH$_3$CO$_2$) (0.13 g, 0.20 mmol) with stirring, whereupon the color changed to deep brown. After addition of sodium methoxide (50 mg, 1 mmol) and NH_4PF_6, the volume was slowly reduced upon standing in an open beaker. The precipitated material was collected by filtration and washed three times with ethanol, once with a small amount of methanol, and then with ether. To a suspension of the isolated brown powder in ethanol (20 mL) was added acetone, until a clear brown solution was obtained. The addition of two drops of concentrated hexafluorophosphoric acid and three drops of hydrogen peroxide (35% solution in water) induced a color change to deep green. After 20 min of stirring, the solution was filtered, and the solvents were allowed to slowly evaporate from an open beaker. The microcrystalline precipitate was collected by filtration, washed with ethanol and ether, and air-dried, yielding an almost black powder. Yield: 0.35 g (68%). R_f(b) = 0. ESI-MS (positive ion, CH_3CN): m/z 2276 ($[[L^{1a}Mn_2O_2](PF_6)_4]^+$), 1065.5 ($[[L^{1a}Mn_2O_2](PF_6)_3]^{2+}$). FT-IR (KBr, cm^{-1}): 3120, 3093, 2969, 2920, 2879, 1603, 1560, 1522, 1483, 1465, 1448, 1427, 1401, 1384, 1349, 1324, 1245, 1187, 1055, 1040, 1004, 957, 840 (PF_6^-), 762 (PF_6^-), 558 (PF_6^-). UV/vis (CH_3CN): λ_{max}/nm ($\epsilon/10^3$ L·mol^{-1}·cm^{-1}) 241 (85), 255 (79), 288 (130), 458 (30), 620sh (2.0). Anal. Calcd for $C_{82}H_{82}N_{18}O_4Ru_2Mn_2(PF_6)_6$: C, 38.39; H, 3.22; N, 9.83; Ru, 7.88; Mn, 4.28. Found: C, 38.89; H, 3.33; N, 9.83; Ru, 7.98; Mn, 4.28.

[L^{1}Mn^{III}](PF$_6$)$_6$. The addition of [Mn$_3$(μ_3-O)(μ-CH$_3$CO$_2$)$_6$(H$_2$O)$_3$](CH$_3$-CO$_2$) (12 mg, 18 μmol) to the deep red solution of [H$_3$L^1](PF$_6$)$_6$ (100 mg, 35 μmol) in a mixture of ethanol (10 mL) and acetone (12 mL) induced a color change to brown. After 15 min of stirring, three drops of hydrogen peroxide (35% solution in water) and three drops of concentrated aqueous hexafluorophosphoric acid were added. The deep brown solution was filtered and the volume slowly reduced in an open beaker. The microcrystalline precipitate was collected by filtration, washed with ethanol and ether, and air-dried to a brown powder. Yield: 60 mg (60%). R_f(a) = 0.06; R_f(b) = 0.50. FT-IR (KBr, cm^{-1}): 3082, 2968, 2924, 2954, 1602, 1567, 1480, 1465, 1447, 1415, 1397, 1376, 1242, 1185, 952, 839 (PF_6^-), 762 (PF_6^-), 558 (PF_6^-). UV/vis (CH_3CN): λ_{max}/nm ($\epsilon/10^3$ L·mol^{-1}·cm^{-1}) 208 (170), 239 (120), 287 (190), 332sh (39), 454 (40). Anal. Calcd for $C_{105}H_{84}N_{21}O_3Ru_3Mn_1$-$(PF_6)_6$: C, 43.25; H, 2.90; N, 10.09; Ru, 10.40; Mn, 1.88. Found: C, 41.98; H, 3.04; N, 9.84; Ru, 10.21; Mn, 1.72.

[L^{1}Mn^{II}Mn^{II}Mn^{II}L^1](PF$_6$)$_{12}$. The deep red solution of [H$_3$L^1](PF$_6$)$_6$ (150 mg, 52 μmol) in a mixture of ethanol (10 mL) and acetone (12 mL) was treated with [Mn$_3$(μ_3-O)(μ-CH$_3$CO$_2$)$_6$(H$_2$O)$_3$](CH$_3$CO$_2$) (20 mg, 31 μmol) and stirred for 1 h. After addition of NH_4PF_6 (150 mg), the solution was filtered, and the solvents were allowed to slowly evaporate from an open beaker. The brown precipitate was isolated by filtration, washed with ethanol and ether, redissolved in ethanol/acetone (50:50, 20 mL), and flushed with argon. After addition of sodium

methoxide (18 mg, 330 μmol), ascorbic acid (21 mg, 100 μmol), and NH_4PF_6 (28 mg), some more $[Mn_3(\mu_3\text{-}O)(\mu\text{-}CH_3CO_2)_6(H_2O)_3](CH_3CO_2)$ ($\sim$3 mg, 5 μmol) was added. The reaction mixture was filtered in an argon atmosphere and its volume slowly reduced in an argon steam. The microcrystalline precipitate was isolated by filtration, washed with argon-flushed ethanol and ether, and dried in vacuo to a deep red powder. Yield: 90 mg (60%). R_f(a) = 0.30; R_f(b) = 0.75. FT-IR (KBr, cm^{-1}): 3076, 2966, 2922, 2853, 1601, 1581, 1526, 1483, 1459, 1446, 1426, 1412, 1393, 1271, 1185, 1106, 1065, 950, 841 (PF_6^-), 762 (PF_6^-), 557 (PF_6^-). UV/vis (CH_3CN): λ_{max}/nm ($\epsilon/10^3$ L·mol^{-1}·cm^{-1}) 210 (320), 242 (290), 288 (330), 325 (79), 387 (59), 436 (61), 457 (61). Anal. Calcd for $C_{210}H_{168}N_{42}O_6Ru_6Mn_3(PF_6)_{12}$: C, 42.85; H, 2.88; N, 9.99; Ru, 10.30; Mn, 2.80. Found: C, 42.17; H, 3.04; N, 10.59; Ru, 9.85; Mn, 2.99.

$[L^2Mn^{IV}](PF_6)_7$. To the red solution of $[H_3L^2](PF_6)_6$ (260 mg, 80 μmol) in ethanol/acetone (50:50, 40 mL) was added $[Mn_3(\mu_3\text{-}O)(\mu\text{-}CH_3CO_2)_6(H_2O)_3](CH_3CO_2)$ (26 mg, 40 μmol). Upon stirring in air for 1 h, the color changed to deep green. After the addition of NH_4PF_6 (0.50 g), the solution was filtered, and the solvents were allowed to slowly evaporate. Dark microcrystals precipitated, which were collected by filtration, washed (ethanol, ether), recrystallized from ethanol/acetone, washed with ethanol, methanol, and ether, and air-dried to a green powder. Yield: 190 mg (69%). R_f(a) = 0.09. ESI-MS (positive ion, CH_3CN): m/z 1572 ($[[L^2Mn^{IV}](PF_6)_5]^{2+}$), 999.7 ($[[L^2Mn^{IV}](PF_6)_4]^{3+}$). FT-IR (KBr, cm^{-1}): 3117, 3082, 3000, 2927, 2854, 1618, 1604, 1571, 1480, 1466, 1446, 1425, 1313, 1245, 1161, 1097, 1077, 841 (PF_6^-), 762 (PF_6^-), 558 (PF_6^-). UV/vis (CH_3CN): λ_{max}/nm ($\epsilon/10^3$ L·mol^{-1}·cm^{-1}) 209 (260), 245 (99), 287 (270), 453 (47), 710 (8.3). Anal. Calcd for $C_{129}H_{120}N_{21}O_6Ru_3Mn_1(PF_6)_7$: C, 45.13; H, 3.52; N, 8.57; Ru, 8.83; Mn, 1.60. Found: C, 44.02; H, 3.71; N, 8.36; Ru, 8.72; Mn, 1.51.

$[L^2Mn^{II}Mn^{II}Mn^{II}L^2](PF_6)_{12}$. $[L^2Mn^{IV}](PF_6)_7$ (100 mg, 29 μmol) and $[Mn_3(\mu_3\text{-}O)(\mu\text{-}CH_3CO_2)_6(H_2O)_3](CH_3CO_2)$ (6 mg, 9 μmol) were dissolved in ethanol/acetone (50:50, 20 mL) and treated with sodium methoxide (16 mg, 290 μmol), which induced a change of the solution color from green to red-brown. After the reaction mixture was flushed with argon, ascorbic acid (15 mg, 85 μmol) was added and the solution filtered under argon. Slow evaporation of the solvents in an argon steam initiated precipitation of red microcrystals, which were collected by filtration in an argon atmosphere, washed with argon-flushed ethanol and ether, and dried in vacuo to a fine red powder. Yield: 70 mg (73%). R_f(a) = 0.26. FT-IR (KBr, cm^{-1}): 3118, 3080, 2963, 2922, 2867, 2838, 1618, 1604, 1484, 1466, 1446, 1425, 1315, 1263, 1241, 1159, 1092, 1027, 972, 841 (PF_6^-), 762 (PF_6^-), 558 (PF_6^-). UV/vis (CH_3CN): λ_{max}/nm ($\epsilon/10^3$ L·mol^{-1}·cm^{-1}) 208 (470), 246 (180), 254sh (180), 287 (500), 453 (87). Anal. Calcd for $C_{258}H_{240}N_{42}O_{12}Ru_6Mn_3(PF_6)_{12}$: C, 46.73; H, 3.86; N, 8.87; Ru, 9.14; Mn, 2.49. Found: C, 45.89; H, 3.86; N, 8.58; Ru, 9.12; Mn, 2.27.

IC990755A